Earth Planets Space, **64**, 613–639, 2012

The existence of cosmic ray sidereal anisotropies of galactic and solar origins with energies lower than 10^4 GeV and their modulation caused by the presumed behavior pattern of the heliomagnetosphere and of its neighboring gaseous matter in interstellar magnetic field

K. Nagashima[1], I. Morishita[2], Z. Fujii[1], S. Mori[3], I. Kondo[4], and R. M. Jacklyn[5]

[1]*Solar-Terrestrial Environment Laboratory, Nagoya University, Chikusa-ku, Nagoya 464-8601, Japan*
[2]*Department of Information Management, Asahi University, 1851 Hozumi, Mizuho, Gifu 501-0296, Japan*
[3]*Physics Department, Shinshu University, Matsumoto, Nagano 390-8621, Japan*
[4]*Institute for Cosmic Ray Research, University of Tokyo, 5-1-5 Kashiwa-no-Ha, Kashiwa 277-8582, Japan*
[5]*Antarctic Division, Department of Science and Technology, Kingston, Tasmania, Australia*

(Received August 21, 2011; Revised February 13, 2012; Accepted February 26, 2012; Online published August 16, 2012)

It is shown that the sidereal anisotropy (S_iA) of cosmic rays (CRs) with energies smaller than 10^4 GeV consists of three kinds: one (GA) is of galactic origin from the direction Φ_G ($\alpha_G = 0$ hr; $\delta_G = -20^\circ$), and the other two (tail-in TA and nose-in HA) are of solar origin from the respective directions Φ_T ($\alpha_T = 6$ hr; $\delta_T \sim -24^\circ$) and Φ_H ($\alpha_H = 18$ hr; $\delta_H > 0^\circ$) and supposed to be produced by the acceleration of CRs on the tail and nose boundaries of the heliomagnetosphere (HMS). This conclusion was arrived at in 1995 after a long-term delay since the beginning of CR observations in the early 20-th century. This delay was mainly due to the inconsistency among observations caused by the belief that the sidereal anisotropy must be unidirectional in space. The inconsistency has been solved at least qualitatively by the discovery of GA and TA. These anisotropies, including also HA, are subject, respectively, to their proper solar modulations in the HMS characterized by a polarity reversal every 11 years of the solar polar magnetic field and solar activity dependence with an 11-year periodicity. By using these modulation patterns, the origins of the three anisotropies have been determined. TA and HA thus determined inversely produce the following kinds of evidence and problems in the HMS: (1) the structure of the HMS, (2) acceleration of CRs on the boundary of the HMS, (3) CR Lens Effect of the HMS for the sharp concentration of TA and HA, (4) the proper motion (V_{HMS}) of the HMS relative to neighboring stars, (5) the proper motion of interstellar gaseous matter (including the magnetic field) relative to neighboring stars, and (6) the existence of the Subordinate HMS surrounding the HMS for the explanation of the duality of the motion of the HMS and also of the absence of the Compton-Getting (C-G) effect on the HMS. The present paper not only presents a brief summary of the studies of CR sidereal anisotropy made by many researchers during the 20th century leading to the present understanding, but also presents some problems to open up a new vista of the future.

Key words: Cosmic rays (CR), sidereal anisotropy, heliomagnetosphere (HMS), interstellar matter (ISM), Compton-Getting effect, motion of the HMS, motion of ISM, acceleration of CRs, cosmic ray lens effect.

1. Introduction

The sidereal anisotropy S_iA of CRs has been inferred indirectly from observations of the sidereal daily variation ($\mathbf{S_iD}$) on the ground ever since the discovery of CRs (e.g. Forbush, 1937a, b, 1939). Recently, due to greatly improved observational methods, the direct observation of S_iA has become possible in the high-energy region by observations with cosmic ray and gamma-ray detectors (e.g. Amenomori *et al*., 2004, 2005; Guillian *et al*., 2007; Abdo *et al*., 2008; Abbasi *et al*., 2010). This method is, however, not applicable to S_iA in the lower energy region as cosmic rays cannot maintain their direction hindered by the influence of the heliomagnetic and geomagnetic fields. In such a low-energy region, $\mathbf{S_iD}$, with the frequency 366 cycles/yr must be detected under the following difficult condition that it is always superposed by the solar daily variation ($\mathbf{S_oD}$) with the adjacent frequency of 365 cycles/yr produced inside the HMS and disturbed by the daily variations of the Earth's atmospheric pressure, temperature and wind velocity. If $\mathbf{S_oD}$ is constant, its yearly average in units of sidereal time, called the spurious sidereal daily variation ($\mathbf{SS_iD}$), becomes zero and does not affect $\mathbf{S_iD}$. Practically, however, as $\mathbf{S_oD}$ is supposed to be almost always disturbed by various kinds of noises, the elimination of $\mathbf{SS_iD}$ is indispensable. In addition to such indirect influences upon $\mathbf{S_iD}$, some of the HMS-phenomena, which directly influence $\mathbf{S_iD}$, have been discovered successively during a long elapsed time, such as the polarity reversal every 11 years of the solar polar magnetic field. It is not an exaggeration to say that the history of the study of $\mathbf{S_iD}$ in the low-energy region ($\leq 10^4$ GeV) has been the history of the study of the direct and in-

Copyright © The Society of Geomagnetism and Earth, Planetary and Space Sciences (SGEPSS); The Seismological Society of Japan; The Volcanological Society of Japan; The Geodetic Society of Japan; The Japanese Society for Planetary Sciences; TERRAPUB.

doi:10.5047/eps.2012.02.004

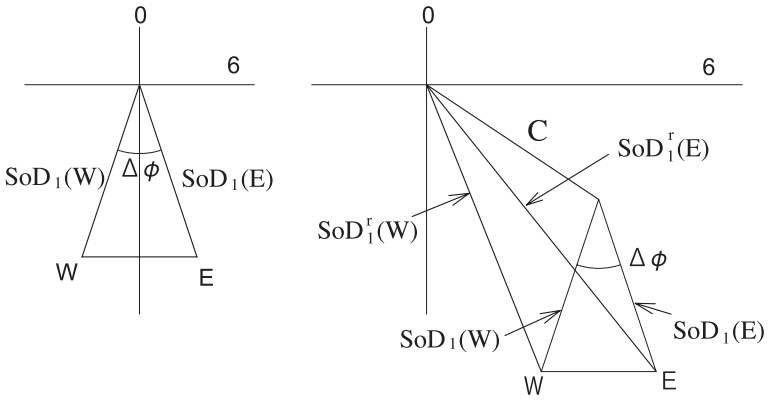

Fig. 1. Elimination of $\mathbf{SS_iD}$ by east- and west-ward CR telescopes with the same zenith angle (Elliot, 1952).

direct influences upon $\mathbf{S_iD}$. In the following, we present a brief summary of the study of S_iA of CRs made by many researchers with a dedicated attention to the direct and indirect influences in order to reach a better understanding of the nature of S_iA and the features associated with it.

2. Influence of SS_iD on S_iD

The attempt to eliminate $\mathbf{SS_iD}$ from the observed $\mathbf{S_iD}$ of CRs has continued ever since the observation of $\mathbf{S_iD}$ began in the early 20th century. Besides the well-known atmospheric influence on $\mathbf{S_iD}$ (e.g. Myssowsky and Tuwim, 1928; Sekido, 1943; Duperier, 1944, 1949; Olbert, 1953; Jacklyn, 1954; Trefall, 1955; Dorman, 1957; Wada, 1960), some of the elimination methods are presented in advance to simplify the following discussion on $\mathbf{S_iD}$.

Type-1.—The East-West difference method.

An atmospheric correction method was proposed by Elliot in 1952, which uses two CR telescopes at a station pointing, respectively, east- and west-ward with the same zenith angle. The elimination method is illustrated by the configuration of the solar diurnal harmonic vectors $\mathbf{S_oD_1}$(E) and $\mathbf{S_oD_1}$(W) with the same amplitude observed by the telescopes as shown in Fig. 1. The two vectors at the left side do not contain the atmospheric effect. The phase difference $\Delta\phi$ between the two vectors is the geographical longitudinal difference and the direction of the anisotropy is 12 hr in this case. If the unknown vector $\mathbf{C}$ due to the atmospheric effect common to the two telescopes is superposed on $\mathbf{S_oD_1}$(E) and $\mathbf{S_oD_1}$(W), the resultant vectors $\mathbf{S_oD_1^r}$(E) and $\mathbf{S_oD_1^r}$(W) are expressed on the right side. The direction of the anisotropy is obtained by rotating the phase of the difference vector ($\mathbf{S_oD_1^r}$(E)–$\mathbf{S_oD_1^r}$(W)) clockwise by 90°. The unknown vectors $\mathbf{C}$, $\mathbf{S_oD_1}$(E) and $\mathbf{S_oD_1}$(W) are derived by constructing the isosceles triangle with the base $|\mathbf{S_oD_1^r}(\mathrm{E}) - \mathbf{S_oD_1^r}(\mathrm{W})|$ and the top angle $\Delta\phi$ as shown in the figure. This method is suitable for the elimination of the atmospheric effects as far as the effects contained in the two telescopes are approximately equal to each other. This method was applied to the observation of the sidereal diurnal harmonic vector $\mathbf{S_iD_1}$ by the Ottawa Horizontal Muon Array (OHMA), (Bercovitch and Agrawal, 1981; Bercovitch, 1984). This method was also applied to $\mathbf{S_oD_1^o}$(E) and $\mathbf{S_oD_1^o}$(W) observed with two directional air shower telescopes (E $\sim 10^4$ GeV) at Mt. Norikura (36°N; 138°E) which succeeded in detecting $\mathbf{S_oD_1}$ from the direction of the 6 hr local solar time, which is produced by the C-G effect due to the Earth's rotation around the Sun relative to the interplanetary cosmic-ray gas (Compton and Getting, 1935; Nagashima *et al.*, 1989).

Type-2.—The Farley-Storey method.

This method was proposed by Farley and Storey in 1954, and eliminates the influence of the annual variation of the amplitude of $\mathbf{S_oD_1}$ from the observed $\mathbf{S_iD_1^o}$ by the following frequency modulation method (FMM). If the amplitude $|\mathbf{S_oD_1}|$ with a frequency of 365 cycles/yr is subject to an annual modulation with a frequency of 1 cycle/yr, the modulated $\mathbf{S_oD_1}$ can be decomposed into three kinds of variation $\mathbf{S_iD_1^f}$, $\mathbf{S_oD_1^f}$ and $\mathbf{AS_iD_1^f}$ with their respective frequencies 366, 365 and 364 cycles/yr as shown on the respective harmonic diagrams S_i, S_o and AS_i in Fig. 2. $\mathbf{AS_iD_1^f}$, called the anti-sidereal diurnal variation, is a newly-defined variation in the new time scale called the anti-sidereal time t_{AS_i} (0 hr–24 hr) and normalized to the other times t_{S_i} and t_{S_o} at the September equinox. The vectors shown on AS_i- and S_i-harmonic diagrams express, respectively, $\mathbf{AS_iD_1^f}$ and $\mathbf{S_iD_1^f}$ with the same amplitude and the respective phases at the September equinox. These vectors, after a parallel transformation to the top of $\mathbf{S_oD_1^f}$ on the S_o-diagram, are axis-symmetric to each other with respective to the $\mathbf{S_oD_1^f}$-axis and rotate, respectively, clockwise and anti-clockwise with the angular velocity $\omega\,(2\pi/\mathrm{yr})$, starting from the September equinox, and the resultant of the three vectors at a time expresses the annual variation of the original $\mathbf{S_oD_1}$. The undetectable $\mathbf{S_iD_1^f}$, supposed to be contained in the observed $\mathbf{S_iD_1^o}$, can be eliminated by using the vector derived from the axis-symmetric inversion of $\mathbf{AS_iD_1^f}$ with respect to the $\mathbf{S_oD_1^f}$-axis. This elimination method has been called the Farley-Storey correction method (Farley and Storey, 1954; Jacklyn, 1962). The application of this method to observations was made frequently in those days though it was not certain whether or not the seasonal modulation of $\mathbf{S_oD_1}$ would belong to the type stated in the above. However, this method will be used later successfully to find the annual variation of $\mathbf{S_iD_1}$ (instead of $\mathbf{S_oD_1}$) produced by S_iA, which is supposed to keep its direction (α, δ) through a year, but vary its amplitude with the maximum and minimum, respectively, at the Earth's orbital location, where the Sun has the same or opposite direction to the source of S_iA,

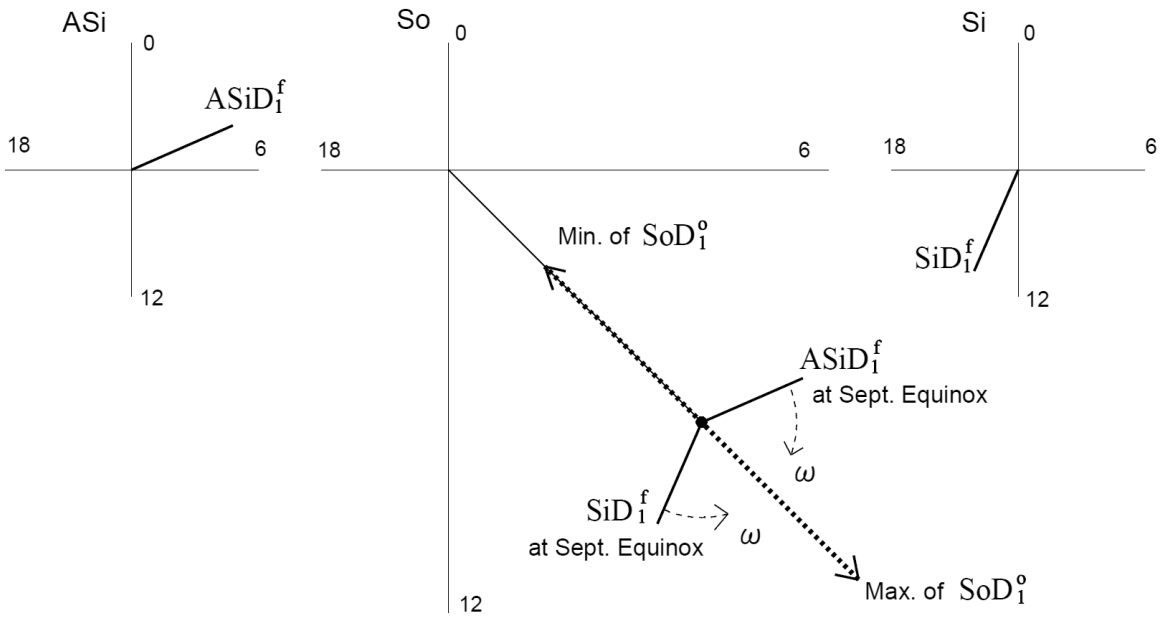

Fig. 2. The Farley-Storey method for the elimination of $\mathbf{SS_iD}$ (Farley and Storey, 1954).

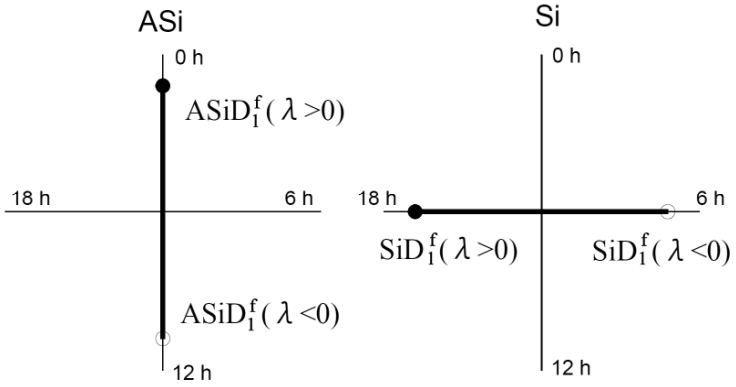

Fig. 3. The CSSA method for the elimination of $\mathbf{SS_iD}$ produced by stationary $\mathbf{S_oD}$ (Nagashima and Ueno, 1971).

and a significant seasonal variation would also be expected because of the Sun's strong magnetic field. In this case, the annual variation of $\mathbf{S_iD_1}$ is decomposed into three vectors $\mathbf{S_oD_1^f}$, $\mathbf{S_iD_1^f}$ and $\mathbf{ES_iD_1^f}$ expressed respectively on the harmonic diagrams S_o, S_i and ES_i. The newly-introduced $\mathbf{ES_iD_1^f}$ is called the extended sidereal diurnal variation with the frequency 367 cycles/yr and will be used later for the determination of the annual variation of S_iA (Nagashima *et al.*, 1998, called hereafter Ref. 3).

Type-3.—Correction for stationary solar anisotropy (CSSA).

In this section, a method is applied that is effective for the elimination of $\mathbf{SS_iD}$ produced by the annual variation of the stationary axis-symmetric S_oA with the direction along the heliomagnetic field (9 hr–21 hr). The annual variation of $\mathbf{S_oD_1}$ is produced from that of the second term of the spherical harmonic series of S_oA owing to the Earth's rotation around the Sun. $\mathbf{S_oD_1}$ is decomposed into the three vectors $\mathbf{S_iD_1^f}$, $\mathbf{S_oD_1^f}$ and $\mathbf{AS_iD_1^f}$ by the FMM. $\mathbf{S_iD_1^f}$ and $\mathbf{AS_iD_1^f}$ at the geographic latitude (λ), shown on the respective harmonic dials in Fig. 3, have the same amplitude proportional to $|\cos\lambda \cdot \sin\lambda|$ and reverse their directions for the sign change of $\sin\lambda$. $\mathbf{S_iD_1^f}$ can be obtained by rotating the corresponding $\mathbf{AS_iD_1^f}$ anticlockwise by 90° and used for the elimination of the influence of the annual variation of $\mathbf{S_oD_1}$ from the observed $\mathbf{S_iD_1^o}$ (Nagashima and Ueno, 1971). This correction method is called CSSA hereafter. Or, if two stations in the N- and S-hemispheres are conjugate to each other with respect to $|\lambda|$, p_c (the geomagnetic cut-off rigidity) and E_m (the CR median energy), the corrected $\mathbf{S_iD_1}$ multiplied by a factor 2 can be obtained by adding the observed $\mathbf{S_iD_1^o}$(N) and $\mathbf{S_iD_1^o}$(S) without decomposing the three vectors $\mathbf{S_iD_1^f}$, $\mathbf{S_oD_1^f}$ and $\mathbf{AS_iD_1^f}$ at each station, as $\mathbf{S_iD_1^f}$(N) is equal to $-\mathbf{S_iD_1^f}$(S). This method is called the simplified CSSA.

It is noted here that although the 2nd term of the spherical harmonic series of S_oA in the above was introduced for the explanation of the observed solar semi-diurnal variation, without any theoretical verification of the existence of such a distribution in space in those days, it seemed to be useful also for an explanation of the $\mathbf{SS_iD}$. The existence of the term has recently been confirmed theoretically (Munakata

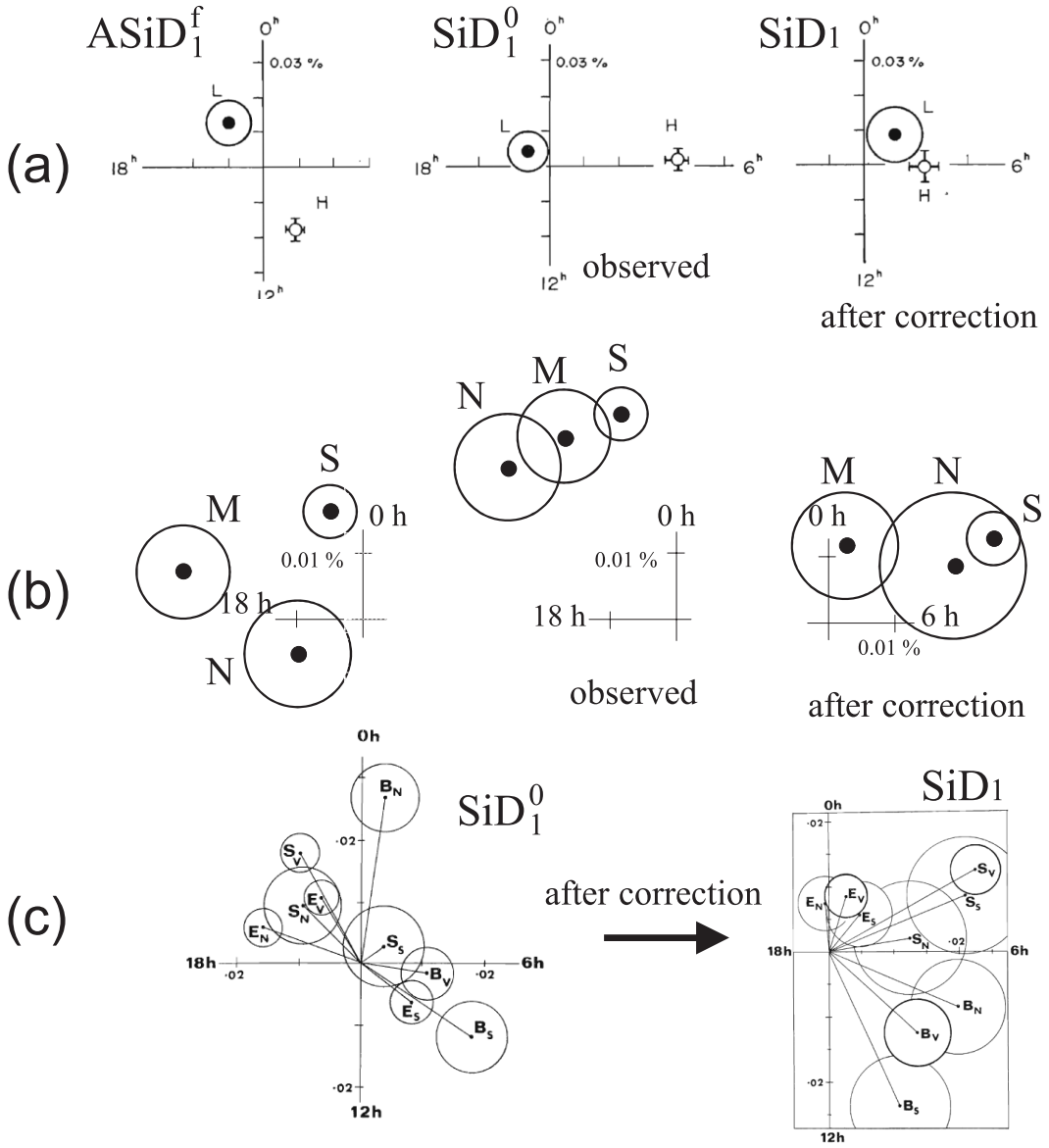

Fig. 4. Elimination of $\mathbf{S_iD_1^f}$ from $\mathbf{S_iD_1^o}$ by using $\mathbf{AS_iD_1^f}$ according to the CSSA method. The corrected vector $\mathbf{S_iD_1}$ is on the right. (a) Underground CR intensities at London (L) and Hobart (H), (Nagashima *et al*., 1985); (b) those at Sakashita (S), Misato (M) and Nagoya (N) at sea level; (c) those at Embudo (E), Socorro (S) and Bolivia (B). The telescopes point vertical (V), North (N) and South (S) at each location and only the observed vectors and, on the right, the corrected vectors, as shown. The amplitude scale is in percent.

and Nagashima, 1986) on the basis of the CR diffusion-convection theory in the HMS (Gleeson and Axford, 1967; Jokipii and Kopriva, 1979). It is also noted that the CSSA method shown in Fig. 3 was obtained in 1971 on the assumption that the solar modulation axis coincides with the solar magnetic dipole axis. The rigorous treatment of the solar modulation in considering the difference of the axes was made by Tatsuoka and Nagashima in 1985 (Nagashima *et al*., 1983b; Tatsuoka and Nagashima, 1985) and the decomposed vectors were obtained as follows (Nagashima *et al*., 1985).

		phase (hr)	
	amplitude	N-hemisphere	S-hemisphere
$\mathbf{S_iD_1^f}$	0.290 η_2	18.73	6.73
$\mathbf{AS_iD_1^f}$	0.306 η_2	23.26	11.26,

where η_2 is the magnitude of the second term of the spherical harmonics. The corrections for those data after 1985 have been based on the revised data shown in the above. Several examples of the correction effect are shown in the following.

Ex. 1—Some correction effects, shown in Fig. 4, indicate that almost all the $\mathbf{S_iD_1^o}$s with the phase in the 4th quadrant (18 hr–24 hr), observed by telescopes pointing to the northern hemisphere, change their phases to the 1st quadrant (0 hr–6 hr) indicating that the $\mathbf{S_iD_1^o}$s contain a very large $\mathbf{SS_iD}$. In Figs. 4(a) and 4(b), the process of the correction method is shown.

Ex. 2—The correction would produce a serious influence on the interpretation of the sidereal anisotropy. The following is another example. In 1966, the bi-directional sidereal anisotropy model was presented by Jacklyn (1966), which was the first concrete anisotropy model ever derived from the observations of sidereal diurnal ($\mathbf{S_iD_1^o}$), and

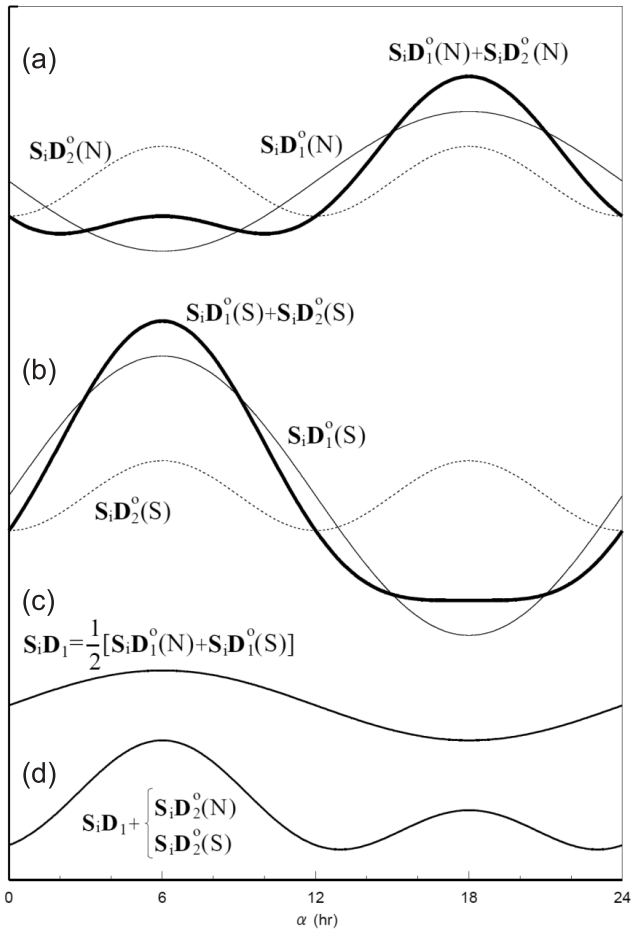

Fig. 5. Schematic diagrams for the explanation of the bi-directional sidereal anisotropy presented by Jacklyn (1966) which used the underground muon telescopes at Budapest (47°N) and Hobart (43°S) and its disappearance by the CSSA correction method.

semi-diurnal ($\mathbf{S_iD_2^o}$), variations by the underground muon telescopes at the northern and southern stations Budapest (47°N) and Hobart (43°S) in the period 1959–1962. The outline of his result is explained by the schematic diagram of the observation in Figs. 5(a) and (b). In it, the resultant of the observed $\mathbf{S_iD_1^o}$ and $\mathbf{S_iD_2^o}$ expressed by dotted curve shows a sharp peak at 18 hr in the N-hemisphere and 6 hr in the S-hemisphere, suggesting that some concentrated CRs are arriving, respectively, from opposite directions probably along a straight line. This is called bi-directional anisotropy, being in accord with the L. Davis model for a pitch angle anisotropy of intensity (Davis, 1954). This model was soon afterwards reconfirmed by directional observations in the N- and S-hemispheres, making use of the Cerenkov detecting telescope at Nagoya ($\lambda = 35°$) (Sekido *et al.*, 1968, 1971), and also by the ion-chamber data at the northern and southern stations Cheltenham ($\lambda = 39°$N) and Christchurch ($\lambda = 44°$S), (Nagashima *et al.*, 1968). However, the $\mathbf{S_iD_1^o}$s shown in Figs. 5(a) and (b) were not corrected by the CSSA method which was not known in those days. The real $\mathbf{S_iD_1}$ has been obtained later by adding the conjugate vectors $\mathbf{S_iD_1^o}(N)$ and $\mathbf{S_iD_1^o}(S)$ according to the simplified CSSA, as shown in Fig. 5(c). $\mathbf{S_iD_1}$ is common in both hemispheres and the resultant of $\mathbf{S_iD_1}$ with $\mathbf{S_iD_2^o}(N)$ or $\mathbf{S_iD_2^o}(S)$ produces a sharply concentrated variation with a phase of 6 hr common in both hemispheres, as shown in Fig. 5(d), suggesting the disappearance of the essential properties of the bi-directional anisotropy model.

On looking back to 1971, we notice that we abandoned at that time the most important principle that sidereal anisotropy should be studied by analyzing at least the sidereal diurnal and semi-diurnal variations and then composing them following the procedure which successfully discovered the bi-directional anisotropy. If this principle has been applied at that time, we would have noticed immediately after the disintegration of the bi-directional anisotropy that the diurnal and semi-diurnal variations at Budapest and Hobart had a common peak at 6 hours, in the N- and S-hemispheres, suggesting the existence of a sharply concentrated uni-directional anisotropy from 6 hours, as shown in Fig. 5(d). Because of this failure in 1971, almost 25 years passed before its discovery in 1995 (Ref. 3). It is further noted here that, during this lost period, only one paper was presented, by Cutler and Groom (1991), concerning the study of the sidereal anisotropy by composing the 1st, 2nd and 3rd harmonic components, and a considerably interesting image of the anisotropy was obtained (cf. Ref. 3).

Ex. 3—The simplified CSSA method applied to the conjugate stations Cheltenham ($\lambda = 39°$N) and Christchurch (44°S) is presented in the following. The long-term averages of $\mathbf{S_iD_1^o}$'s at these stations are shown in Fig. 6, together with that at the equatorial station Huancayo ($\lambda = 12°$S),

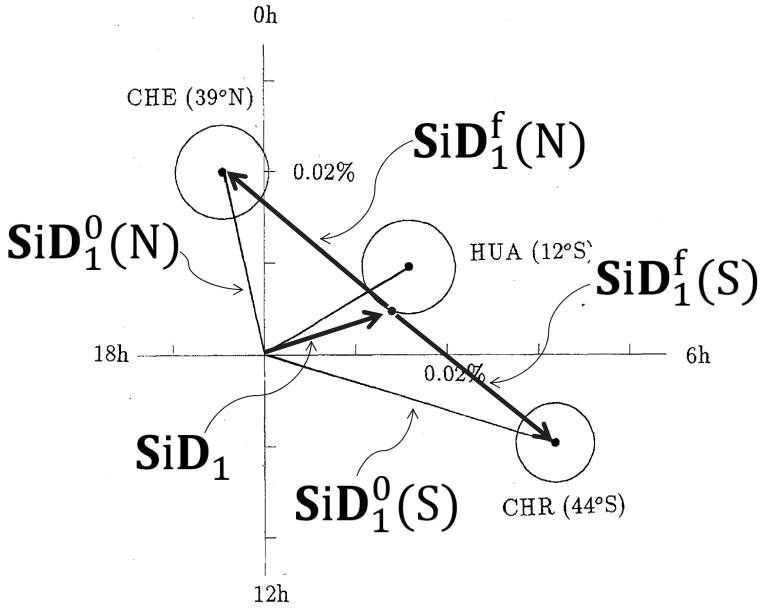

Fig. 6. $\mathbf{S_iD_1}$'s with the error circles observed with the ion chambers at Cheltenham ($\lambda = 39°$N; $\phi = 283°$E; $E_m = 67$ GeV) and Christchurch (44°S; 173°E; 67 GeV) during 1937–1958 and at Huancayo (12°S; 285°E; 62 GeV) during 1936–1959, cited from Nagashima and Mori (1976). These results were derived from the data published by Lange and Forbush (1948, 1957) and Beach and Forbush (1961).

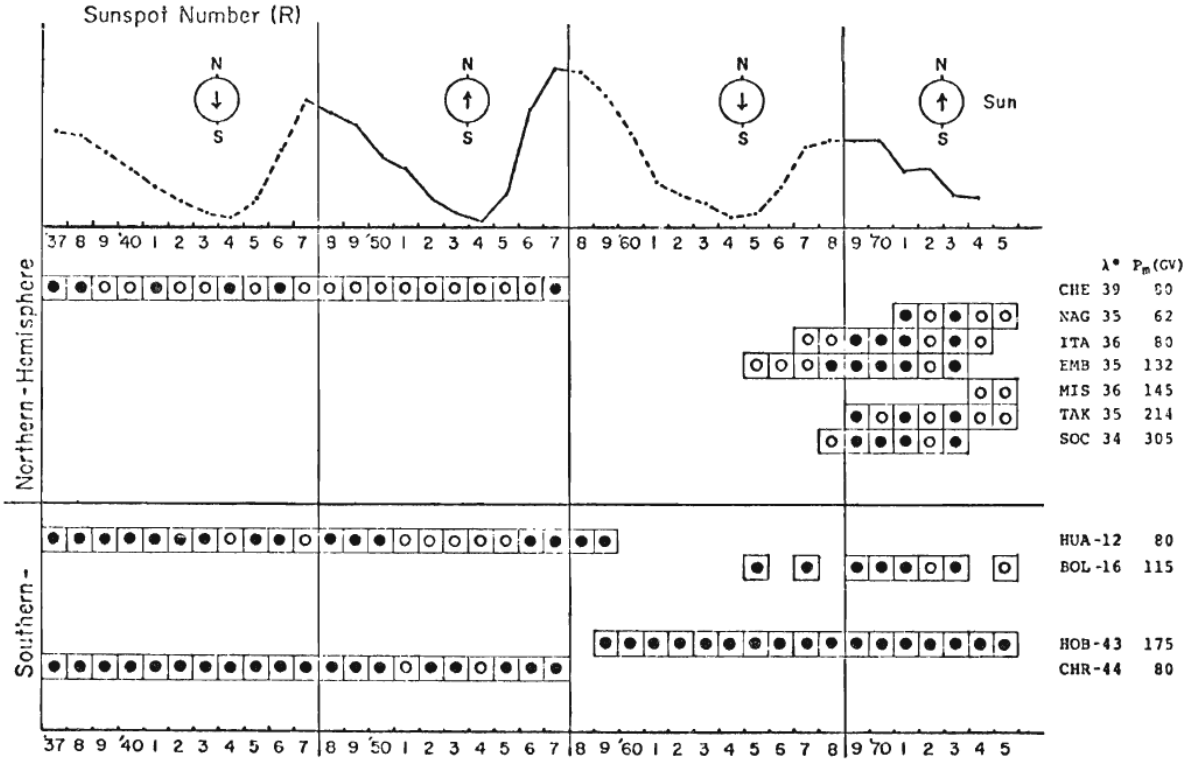

Fig. 7. Time series of phase of $\mathbf{S_iD_1^0}$ without CSSA (Nagashima and Mori, 1976). Solid circle: Morning side (0–12 hr); Open circle: Evening side (12–24 hr); NAG, ITA, MIS and TAK (Ichinose and Murakami, 1976); EMB, SOC and BOL (Swinson, 1976); HOB (Humble and Fenton, 1975; Fenton and Fenton, 1976); CHE, HUA and CHR (Lange and Forbush, 1948, 1957; Beach and Forbush, 1961).

(cf. Ref. 3). In it, the north-south difference of $\mathbf{S_iD_1^0}$'s at Cheltenham and Christchurch is clearly seen. In those days of the analysis (1976), this difference was misinterpreted by Nagashima and Mori (1976) as being due to some north-south asymmetric sidereal vectors being superposed on a common sidereal vector, in spite of the earlier findings of their real origin in 1971 by Nagashima and Ueno. Fortunately, the decomposed vectors $\mathbf{S_iD_1^f}$(N) and $\mathbf{S_iD_1^f}$(S) shown in Fig. 6 can be identified with those derived from the simplified CSSA method at the two conjugate stations Cheltenham and Christchurch. The persistent difference between $\mathbf{S_iD_1}$'s at these stations is shown by their phase dif-

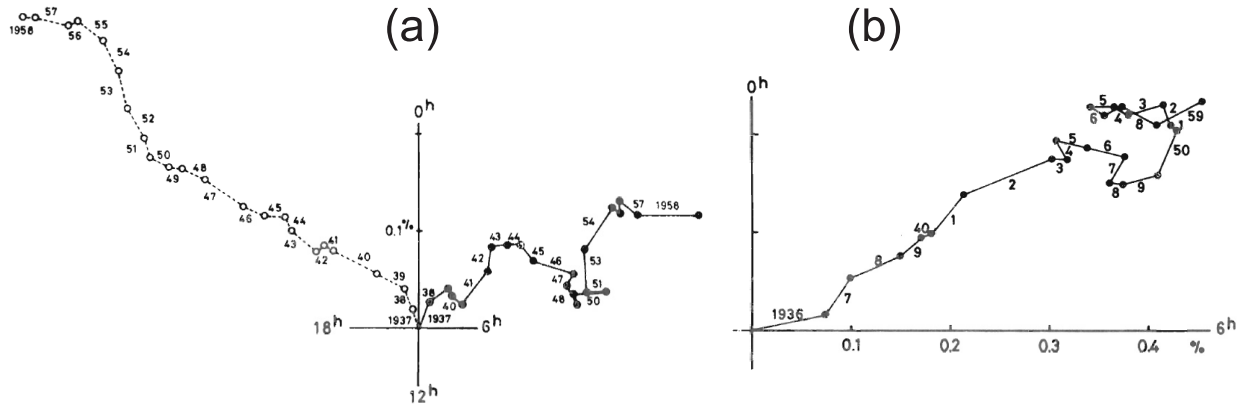

Fig. 8. Summation diagrams $\Sigma \mathbf{S_i D_1}$ (on the right) and $2\Sigma \mathbf{S_i D_1^f}$(N) in Fig. 8(a) and of the yearly vectors, and $\Sigma \mathbf{S_i D_1^o}$(HUA) in Fig. 8(b), of the yearly vectors in Fig. 6.

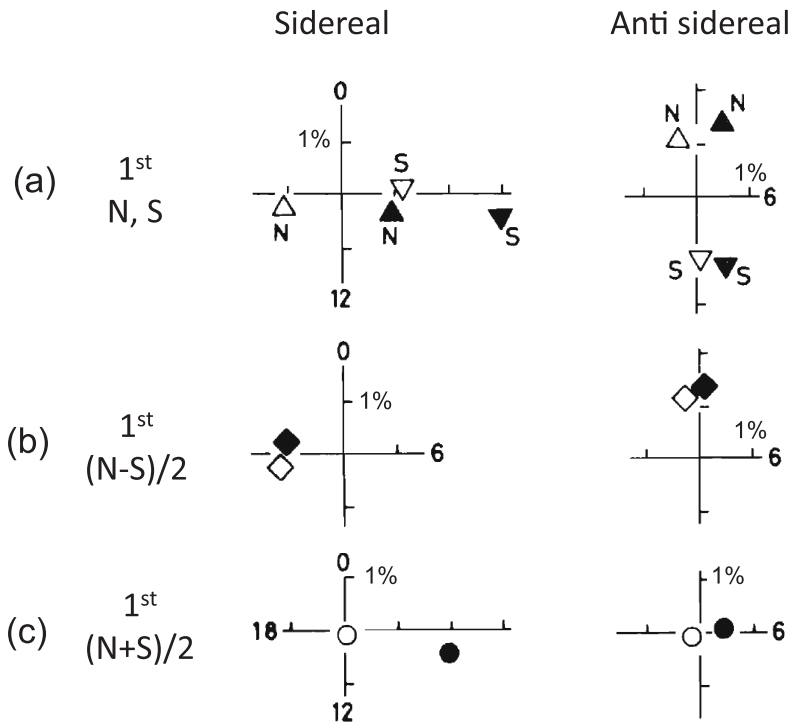

Fig. 9. The elimination of SS_iA from $\mathbf{S_i D_1^o}$ by the modified CSSA method, applied to the conjugate $\mathbf{S_i D_1^o}$(N) and $\mathbf{S_i D_1^o}$(S) artificially produced by averaging, respectively, almost all the northern and southern neutron monitor data (Nagashima *et al*., 1983a, 1984). Black triangles, observed total vectors; open triangles, expected spurious; black circle, corrected vector; open circle, resulting spurious.

ference classified into morning (0–12 hr) and evening (12–24 hr) sides by the open and solid circles in Fig. 7. This asymmetry is very stable as can be seen also in the summation dial of the yearly vectors $\Sigma 2 \times \mathbf{S_o D_1^f}$(N) shown in Fig. 8(a). On the other hand, $\mathbf{S_i D_1}$ almost coincides with $\mathbf{S_i D_1^o}$ at Huancayo, indicating the negligible influence of $\mathbf{S_i D_1^f}$ at the equatorial station Huancayo (cf. Fig. 6). It is emphasized that these two vectors show remarkable yearly fluctuations, especially in the period 1948–1957, of the positive polarity (P-) state of the solar polar magnetic field shown in Fig. 8. Especially, the solar activity minimum period in the P-state seems to be a special epoch for the appearance, or the phase change, of the sidereal anisotropy, which occurs every 22 years. The occurrences of the event have been successively observed in 1954 (Conforto and Simpson, 1957), in 1975–1976 (Swinson, 1976; Nagashima *et al*., 2010) and in 1996 (Nagashima *et al*., 2010).

Ex. 4—The simplified CSSA was applied also to $\mathbf{S_i D_1}$'s and $\mathbf{AS_i D_1}$'s at the conjugate neutron monitor stations in the N- and S-hemispheres which were artificially made by averaging respectively the $\mathbf{S_i D_1^o}$s and $\mathbf{AS_i D_1^o}$s of almost all the data of 473 station-years in the northern stations and 147 station-years in the southern stations in the period of 1958–1979. The averaged $\mathbf{S_i D_1^o}$'s and $\mathbf{AS_i D_1^o}$'s are shown in Fig. 9(a) with the labels N or S. Their sum and difference between the N- and S-hemispheres express respectively $\mathbf{S_i D_1}$, $\mathbf{S_i D_1^f}$, $\mathbf{AS_i D_1^f}$ and those residuals shown in Figs. 9(b) and 9(c). $\mathbf{S_i D_1^f}$ and $\mathbf{AS_i D_1^f}$ in Fig. 9(c) are almost the same in magnitude and their phases are, respectively, in the proper directions of 18 hr and 0 hr in the

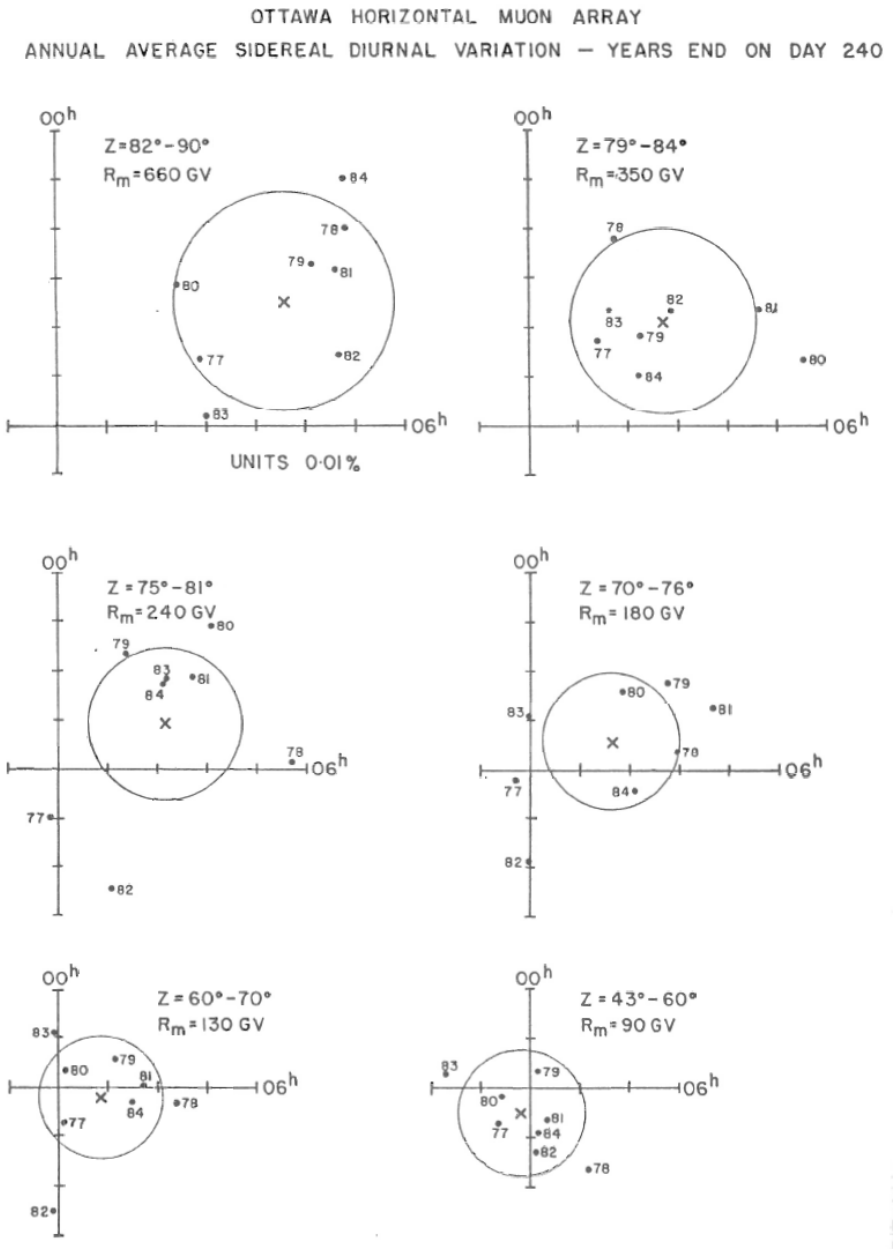

Fig. 10. Energy dependence of $\mathbf{S_iD_1}$ observed Ottawa Horizontal Muon Array (Bercovitch, 1984).

N- and S-hemispheres, justifying inversely the simplified CSSA method applied to the artificial conjugate stations. The phase of the real $\mathbf{S_iD_1}$ is 6.8 ± 0.3 hr and almost coincides with that observed at Hobart (λ 43°S; E_m 184 GeV) as shown in Fig. 4(a). However, the phases at London (λ 52°N; 60 m.w.e.) and those in Figs. 4(a) and 4(b), deviate toward the mid-night side from 6 hrs. The deviation ($\Delta\phi$) increases with the increase of cosmic-ray energy and reaches at the maximum ($\Delta\phi = 6$ hr) in the energy region $\sim 10^4$ GeV observed by air showers at Mt. Norikura (36°N, 133°E) (cf. figure 9 in Ref. 3). Such an energy dependence was found in a wide range of rigidities (90–660 GeV) with the OHMA in the period 1976–1984 by Bercovitch (1984), as shown in Fig. 10.

In spite of such differences in phase in the low- and high-energy regions, the coincidences in phase observed by the neutron monitor (Ex. 4, ~20 GeV, 1983), ion-chamber (Ex. 3, ~67 GeV, 1976) and the underground muon telescope (Ex. 2, ~184 GeV, 1966) seem to suggest the existence of some sidereal anisotropy in the low-energy region in space from $\alpha = 6$ hours (Nagashima *et al.*, 1983a, 1984). But this was not accepted unanimously at that time for the following reasons: (1) the difference of the phases in the low- and high-energy regions mentioned above cannot be explained by the difference between CR deflections produced by the single anisotropy in the HMS, (2) the signal of the anisotropy in the low-energy region (~20 GeV) would be difficult to maintain its shape until its arrival at the Earth because of disturbance in the HMS and therefore the observed $\mathbf{S_iD_1}$ might be some residual of $\mathbf{SS_iD}$, and (3) the CSSA-method was not unanimously accepted in those days. Therefore, it took about another 20 years for the confirmation of such an anisotropy.

Although all the events corrected by the CSSA method do

not directly connect with the image of sidereal anisotropy, they will be used to specify the discussion for the determination of the anisotropy, without any explanation of their complicated derivation process.

3. S_iA in the HMS

Since the discovery of the polarity reversal of the solar polar magnetic field (Babcock, 1959; Howard, 1974a, b), its influence has been discussed actively in considerations of cosmic-ray intensity variations (e.g. Moraal, 1976; Nagashima, 1977 and references therein; Kuzmin *et al.*, 1977; Nagashima and Morishita, 1980a, b; Kota and Jokipii, 1983; Nagashima, 1990 and references therein; Nagashima *et al.*, 1991; Belov, 2000, references therein; Duldig, 2000 and references therein) and the cosmic-ray solar diurnal variation (Duperier, 1946; Thambyahpillai and Elliot, 1953; Gleeson and Axford, 1967; Kota, 1975; Moraal, 1976; Jokipii and Kopriva, 1979; Mori *et al.*, 1981; Bieber and Pomerantz, 1983; Munakata and Nagashima, 1986; Nagashima *et al.*, 1986 and references therein). The observational data of the cosmic-ray sidereal anisotropy, however, were limited in those days, but the theoretical expectation of the polarity dependence has been proposed by many authors in considering the interaction between interstellar and interplanetary magnetic fields, (e.g. Davis, 1954, 1955; Sarabhai and Subramanian, 1966; Schatten and Wilcox, 1969; Marsden *et al.*, 1976; Nagashima and Mori, 1976; Davies *et al.*, 1977; Benko *et al.*, 1979; Krainev, 1981). On the other hand, another approach to study $\mathbf{S_iD_1}$ has been made by putting special emphasis on the behavior of the CR orbits arriving at several specific stations from a specified S_iA, (e.g. Speller *et al.*, 1972; Marsden *et al.*, 1976; Davies *et al.*, 1979). As part of further progress of such studies, the general formulation of the solar modulation of the axis-symmetric S_iA from an arbitrary direction was presented (Nagashima *et al.*, 1982; Nagashima and Morishita, 1983, called hereafter Refs. 1 and 2; Yasue *et al.*, 1985). According to this formulation, $\mathbf{S_iD_1}$ and $\mathbf{S_iD_2}$ produced by this modulation can be expressed respectively by the linear combination of the vectors selected from the eight basic vectors in the geographic coordinate depending on the direction and constituent of S_iA. Hereafter, this formulation of the modulation is called the modulation model. The most characteristic feature of the modulation is that $\mathbf{S_iD_1}$ produced by S_iA from the direction of the equatorial region is greater in the N- state than in the P-state, while, from the direction of the polar region, it is greater in the P-state than the N-state, or becomes almost equal in both states.

As regards observations, on the other hand, Cini-Castagnoli *et al.* (1975) first pointed out that a remarkable phase change from ∼18 hr to 3–6 hr was observed in the sidereal variation only in the Northern hemisphere for the transition from the N-state to the P-state in 1968/69. These stations were London (52°N; p_m = 261 GV), Socorro (34°N; 280 GV) and Torino (45°N; 291 GV). They attributed the phase shift to the change of cosmic-ray orbital deflection in the HMS. This suggestion was supported by Gavril'yev *et al.* (1977), based on the observation at Yakutsk (62°N; 67 GV) in 1958–1975. Ichinose and Murakami (1976) also confirmed the occurrence of the

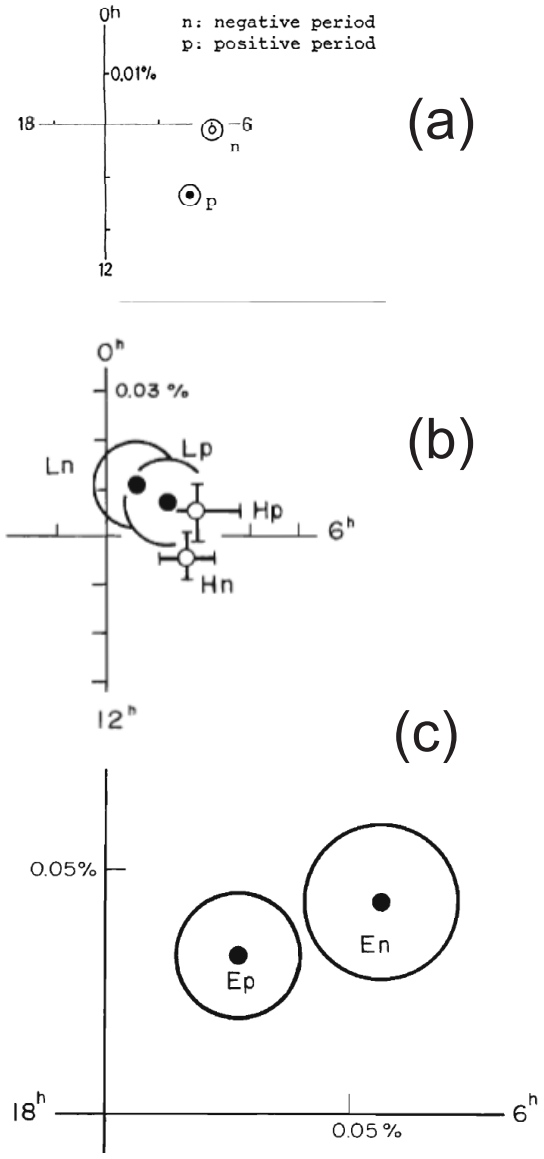

Fig. 11. Polarity dependence of $\mathbf{S_iD_1}$. (a) Neutron in the N-state (n) (1961–1969) and the P-state (1970–1978). (b) London (L) (52°N, 60 m.w.e.) in the N-state (1961–1969; 1981–1982) and the P-state (1970–1978); Hobart (H) (43°S, 36 m.w.e.) in the N-state (1958–1969; 1981–1982) and in the P-state (1970–1980). (c) London equatorially pointing telescope (E) (421 GV) in the N-state (1981–1982) and in the P-state (1970–1978).

shift at Takeyama (35°N; 212 GV), Misato (36°N; 145 GV), Tokyo (36°N; 71 GV) and Nagoya (35°N; 60 GV). They pointed out, however, that these phases were changeable from year to year and another marked phase shift, which occurred in 1973/74, was not attributable to the polarity reversal proposed by Cini-Castagnoli *et al.* According to the modulation model, one can find one vector out of the eight basic vectors which produces the shift from ∼18 hr to 3–6 hr in the northern hemisphere for the transition from the N- to the P-state (1968/69). However, the vector is north-south asymmetric and must produce also a shift inversely from ∼6 hr to 18 hr in the southern hemisphere against the observation (cf. Ref. 2). The polarity dependence was further studied by using the data during a long-term period in order to increase the statistical accuracy. Some of the re-

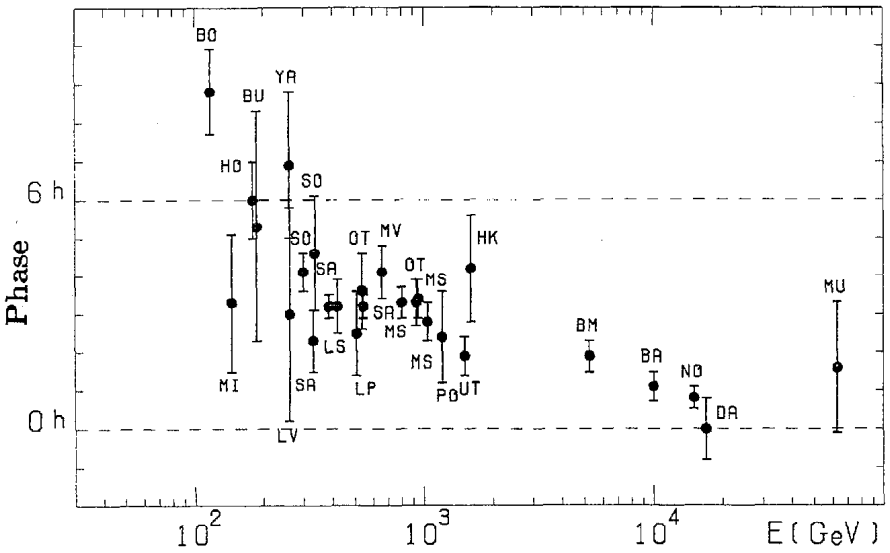

Fig. 12. Energy dependence of the phase of the observed $\mathbf{S_iD_1}$ cited from Ref. 3. All the $\mathbf{S_iD_1}$'s except several in the high-energy region are those of the vertical intensities corrected by the CSSA method, or those for the equatorially directed telescopes which do not require the above correction owing to a negligible influence. BO, Bolivia; SO, Socorro (Swinson and Nagashima, 1985); MI, Misato; HO, Hobart; BU, Budapest; YA, Yakutsk; LO, London (Nagashima *et al.*, 1985 and references therein); SA, Sakashita (Ueno *et al.*, 1990); LS, London (Thambyahpillai, 1983); LP, Laipootah; MV, Matsushiro (Mori *et al.*, 1993); OT, Ottawa (Bercovitch and Agrawal, 1981); MS, Matsushiro (Mori *et al.*, 1989); UT, Utah (Cutler and Groom, 1991); PO, Poatina (Fenton and Fenton, 1975; Humble *et al.*, 1985); HK, Hong Kong (Lee and Ng, 1987); BM, Baksan (Andreyev *et al.*, 1987); BA, Baksan (Alexeenko *et al.*, 1981); NO, Norikura (Nagashima *et al.*, 1989); DA, Norikura, directional air showers (Nagashima *et al.*, 1989) and MU, Musala (Gombosi *et al.*, 1975).

sults are shown in Figs. 11(a), 11(b) and 11(c). The polarity dependence of neutrons in Fig. 11(a), which was obtained by the same method applied to the previous event in Fig. 9, shows some phase difference between the two vectors but does not show any amplitude modulation against the modulation model. The other two cases in Fig. 11(b) and 11(c) also do not show any clear difference in their amplitudes (Nagashima *et al.*, 1985). Furthermore, the multidirectional OHMA mentioned previously could not observe the polarity dependence of the amplitude in the wide energy region (90–660 GeV) although their observation period (1976–1984) was not so long (cf. figures 3 to 8 in Bercovitch, 1984). The discrepancy between the observation and the modulation model concerning the polarity dependence was a serious question in those days. In addition to this difficult problem, there was another difficulty as follows.

The sidereal anisotropies observed at various energy regions did not show a definite direction as pointed out in the previous section. This is called the phase anomaly, hereafter. This anomaly has not been eliminated by the CSSA, nor by an increase of observations and statistical accuracy. The energy dependence of the phases observed at individual stations is shown in Fig. 12 (cf. Ref. 3). These data are selected from many observations in the past on the condition that they finished CSSA, or that this was unnecessary as their telescopes were directed towards the equatorial region. In the low-energy region, the phase is ~6 hr observed by neutrons and the underground muon detector at Hobart (cf. Figs. 9 and 10) and, with an increase of energy, it shifts towards ~0 hr observed by the air showers at Mt. Norikura (36°N, 1.5×10^4 GV), (Nagashima *et al.*, 1989). Such a phase anomaly cannot be explained by the magnetic deflection produced by the modulation model (Ref. 2). The anomaly could be observed, even at a single station, by the OHMA in the energy region (90–660 GV) under the same condition as shown in Fig. 10.

In addition to these problems, the following most important and difficult one must be added. In the northern hemisphere, the phase ϕ_1 of the first harmonic vector $\mathbf{S_iD_1}$ of the sidereal anisotropy S_iA varies from 0 hr to 6 hr depending on the energy; on the other hand, the phase ϕ_2 of the second harmonic vector $\mathbf{S_iD_2}$ is ~6 hr regardless of E_m (Nagashima and Mori, 1976; Fujii *et al.*, 1984; Mori *et al.*, 1989; and references therein). On the contrary, in the southern hemisphere, ϕ_1 and ϕ_2 are all 6 hrs regardless of the energy. The solution for these problems will be discussed in the next section.

In relation to these phenomena, it would be worthwhile to mention that the anomalous enhancement of $\mathbf{S_iD_1}$ in the equatorial zone was observed at Sakashita (540 GeV) by Ueno *et al.* (1984) and at Matsushiro (220 m.w.e.) by Mori *et al.* (1989, 1993), which was not certain whether it is due to the North-South asymmetric distribution, or the equatorial anomaly. Although the anomaly failed to be explained by the unidirectional anisotropy, it is conducive to the determination of GA and TA that follows.

4. GA and TA of Three Kinds of Sidereal Anisotropy in the HMS

A clue to understanding those difficult problems mentioned in the previous section has been obtained by a casual finding of the seasonal variation of $\mathbf{S_iD_1}$ with $\phi_1(t_{S_i})$ ($\alpha = 6$ hours) at Hobart (Nagashima *et al.*, 1995a, b, c). As mentioned previously, the seasonal variation of $\mathbf{S_iD_1}$ (366 cycles/yr) is expressed by the variations with the sideband

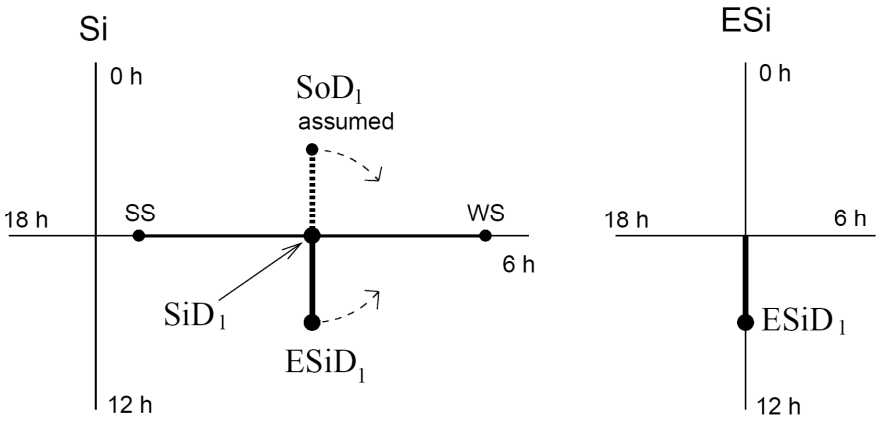

Fig. 13. Schematic representation of the seasonal variation of $\mathbf{S_iD_1}$ and $\phi_i(t_{S_i})$ ($\alpha = 6$ hours) at Hobart (cf. Type 2.—the Farley-Storey method). WS: Winter Solstice; SS: Summer Solstice.

frequencies 365 and 367 cycles/yr, called the solar ($\mathbf{S_oD_1^f}$) and the extended sidereal ($\mathbf{ES_iD_1^f}$) variations. It was found that the $\mathbf{S_iD_1}$ in question contains $\mathbf{ES_iD_1^f}$ with the phase of $t_{ES_i} = 12$ hours, suggesting the existence of a seasonal variation of some sidereal anisotropy S_iA responsible for $\mathbf{S_iD_1}$. The seasonal variation of S_iA must be of the Farley-Storey type as the declination δ_{S_i} of S_iA is constant, contrary to that (δ_{S_o}) of S_oA of solar origin. The relative configuration between $\mathbf{ES_iD_1^f}$ and the average vector $\mathbf{S_iD_1}$ is shown in Fig. 13 (cf. Fig. 2 and cf. Ref. 3). The configuration can be explained if S_iA is subject to a seasonal variation with its maximum and minimum, respectively, at the December solstice ($\alpha = 6$ hours) and the June solstice ($\alpha = 18$ hours) when the Earth is located where the Sun has the same, or opposite, direction to the source of S_iA, and a significant seasonal variation would also be expected because of the Sun's strong magnetic field. The dashed vector in Fig. 13 is another anticipated sideband vector ($\mathbf{S_oD_1^f}$) of S_iA. Although it cannot be observed explicitly by the disturbances of a large $\mathbf{S_oD_1}$, it nevertheless disturbs $\mathbf{S_oD_1}$, like the seasonal variation ($\mathbf{S_iD_1^f}$) of $\mathbf{S_oD_1}$ disturbs $\mathbf{S_iD_1}$ mentioned earlier. It will be shown later that the influence of the disturbance is not negligibly small.

As pointed out earlier, the evidence of the existence of an anisotropy similar to S_iA in the above should have been recognized in the period when the bi-directional anisotropy observed at Budapest and Hobart was reported (cf. Fig. 5). In fact, the $\mathbf{S_iD_1^o}$ and $\mathbf{S_iD_2^o}$ observed, respectively, at the two stations finally produced a sharply-concentrated $\mathbf{S_iD}$, with the phase of 6 hr common in both hemispheres supposed to have been produced by a S_iA (cf. Fig. 5(d)). The S_iA thus derived by the two different methods as above is also supported by the previous observations with neutron monitors and ion-chambers shown in Figs. 6 and 9(b) and also by the observations (1983–1993) at Mawson (68°S, 63°E) with the telescope pointing in the same direction as the Hobart telescope (43°S), which showed the same sidereal diurnal vector as Hobart (Jacklyn, 2000). These evidences inevitably require another anisotropy mainly responsible for the sidereal variations observed in the northern hemisphere. This idea was the key to finding two kinds of cosmic-ray sidereal anisotropy of galactic and solar origins (Nagashima *et al.*, 1995a, b, c). In order to confirm the existence of these two kinds of anisotropy, the latitude and energy dependence of the $S_iD(t_{S_i})$'s at several stations are shown on an hourly basis in Fig. 14(a) (cf. Ref. 3). At the top of Fig. 14(a), the air shower observation of $S_iD(t_{S_i})$ at Mt. Norikura is also shown for comparison, which is compatible with that observed at Baxan (Alexeenko and Navarra, 1985). In Fig. 14(b) on the right side, some uncorrected $S_iD^o(t_{S_i})$'s and their associated anti-sidereal variations $AS_iD(t_{AS})$'s, observed with three telescopes looking, respectively, in geographic latitudes $\lambda > 0°$, $\sim 0°$ and $< 0°$, are plotted in order to show the influence of $S_oD(t_{S_o})$. In Fig. 14(b), $S_iD^o(t_{S_i})_{SAK}$, with positive λ, has two peaks near 18 and 6 hours. Once the correction is applied, the larger peak at 18 hours vanishes into a flat plateau, but the smaller one is rather enlarged as shown in Fig. 14(a). The same can be said of $S_iD(t_{S_o})^V_{NAG}$ (cf. Fig. 14(a)). On the other hand, in the case of the equatorially pointing S_{SAK} telescope, the $S_iD(t_{S_i})$'s before, and after, the correction do not differ much from each other owing to an almost flat $AS_iD(t_{AS})$ as expected, and show a good similarity with $S_iD(t_{S_i})^V_{NAG}$. At the southern station Hobart (43°S), on the other hand, the correction does not change the form of $S_iD^o(t_{S_i})$ so drastically as in the N-hemisphere but only reduces its peak at $\sim$6 hours and flattens the minimum.

The sidereal variations in Fig. 14(a) are characterized by narrow peaks and/or deep valleys, whose centers are almost at 6 and 12 hours, respectively. The peaks almost disappear for the northernmost pointing N_{NAG} telescope, while the valleys lose their similarity to others for the southernmost V_{HOB} telescope. This suggests that the peaks and valleys are of a different origin. It is emphasized that all the valleys, except at Hobart, are very similar to that of the air showers (F3) with almost no phase difference. Furthermore, it cannot be emphasized too much that the entire time profile of $S_iD(t_{S_i})^N_{NAG}$ for the northernmost looking N_{NAG}-telescope almost completely coincides in shape with that of $S_iD(t_{S_i})^{F3}_{NOR}$ as can be seen by their superposition in Fig. 15. This implies that the sidereal anisotropy, observed by the air showers with the median energy ($E_m \sim 10^4$ GeV), can be observed even at very low energies ($E_m \sim 60$ GeV) without any deformation in shape and with almost no phase dif-

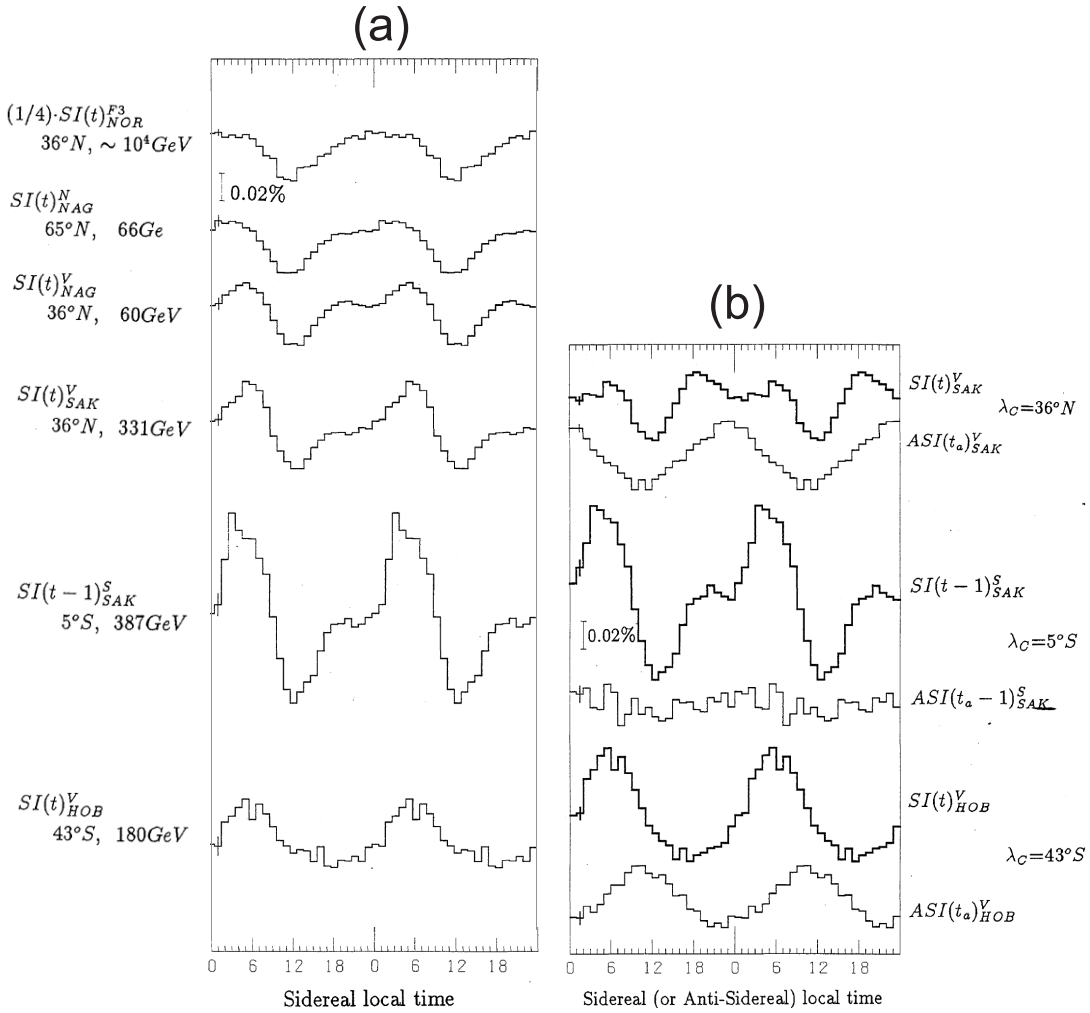

Fig. 14. (a) Latitude and Energy dependence of $S_iD(t_{S_i})$, suggesting the existence of two kinds of sidereal anisotropies $G(t_{S_i})$ and $T(t_{S_i})$ respectively from $\alpha = 0$ hr and 6 hr and (b) the three of them without CSSA, together with their associated $AS_iD(t_{AS})$, to show their influence on $S_iD^o(t_{Si})$.

ference from the air showers. Other $S_iD(t_{S_i})$s except for $S_iD(t_{S_i})^V_{HOB}$ also coincide with that of the air showers fairly well except for the appearance of the peak of another origin, as can be seen by the examples of the superposed curves in Fig. 15. A sidereal variation of galactic origin, which has a broad plateau and a narrow valley with its minimum near 12 hours, is characterized by its constituent first (24 hours) and second (12 hours) harmonic vectors $\mathbf{GD_1}$ and $\mathbf{GD_2}$, with their respective phases 0 hours and 6 hours, and is called the G variation or $G(t_{S_i})$, hereafter. According to the previous analysis of $G(t_{S_i})$ of the air showers (Nagashima *et al.*, 1989), the space distribution of the galactic anisotropy responsible for $G(t_{S_i})$ can be expressed by a deficit flux confined in a narrow cone with the half opening angle $\chi = 57°$ from the direction of Φ_G ($\alpha_G = 12$ hours and $\delta_G = 20°$). On the other hand, the variation, characterized by a narrow peak with a maximum at ~6 hours, can be separated from $G(t_{S_i})$ by a similar process shown in Figs. 15–16. The result is shown in Fig. 16.

This variation is characterized by its constituent first and second harmonic vectors $\mathbf{TD_1}$ and $\mathbf{TD_2}$ with their common phase of 6 hours, and is called the T-variation, or $T(t_{S_i})$, whose origin is called T-anisotropy or TA. It is emphasized that as the sidereal diurnal variation $\mathbf{S_iD_1}$ is the resultant of $\mathbf{GD_1}$ and $\mathbf{TD_1}$, its phase varies from 0 hours to 6 hours depending on the contribution of the two kinds of component, while the sidereal semi-diurnal variation $\mathbf{S_iD_2}$ has a constant phase of 6 hours as $\mathbf{GD_2}$ and $\mathbf{TD_2}$ have a common phase of a constant value of 6 hours regardless of their energies. It is noteworthy that these variations make it possible to derive $\mathbf{GD_1}$ and $\mathbf{TD_1}$ inversely from the observed $\mathbf{S_iD_1}$ by taking its projections respectively along the 0 hr-axis and the 6 hr-axis of the harmonic dial. Some examples of the energy dependence of the amplitude of $\mathbf{GD_1}$ and $\mathbf{TD_1}$ is shown in Fig. 17, which is derived from those $\mathbf{S_iD_1}$'s whose phases are shown in Fig. 12 (Ref. 3).

Nagashima *et al.* (1998) were indicating that at energies less than 10^4 GeV the amplitude of TA was decreasing with increasing energy, giving strength to the conclusion that TA was of solar origin. Remarkably, since that time it has been reported from a number of advanced experiments that TA continues to exist at energies in the multi-TeV region, raising new questions regarding the evidence for the solar origin of TA.

According to the previous analysis (cf. Ref. 3), the space distribution of the T-anisotropy (or TA) responsible for these $T(t_{S_i})$'s can be expressed by a directional excess flux confined in a cone with a half opening angle (χ_T) of ~68°

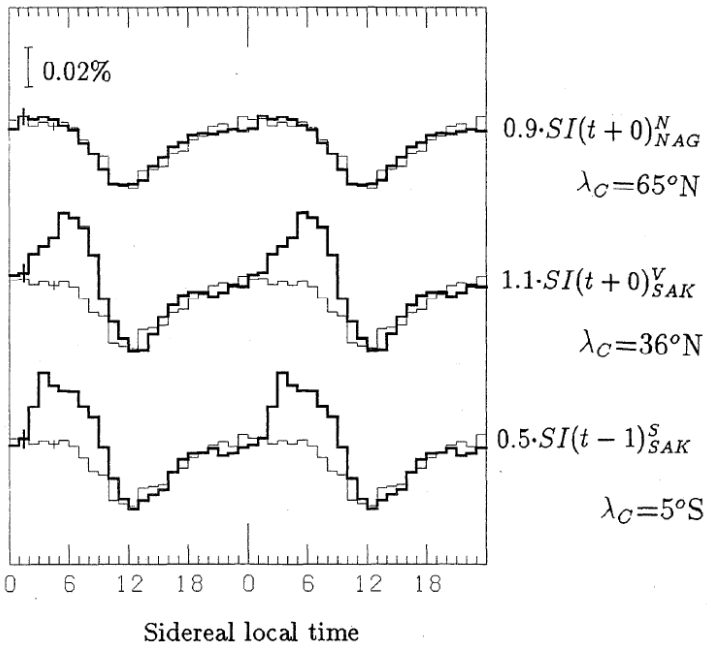

Fig. 15. Similarity of the air showers (light line) due to GA with the $S_iD(t_{S_i})$ (dark line) except for the sharply-concentrated variation due to TA, produced by adjusting their magnitude but without their phase change.

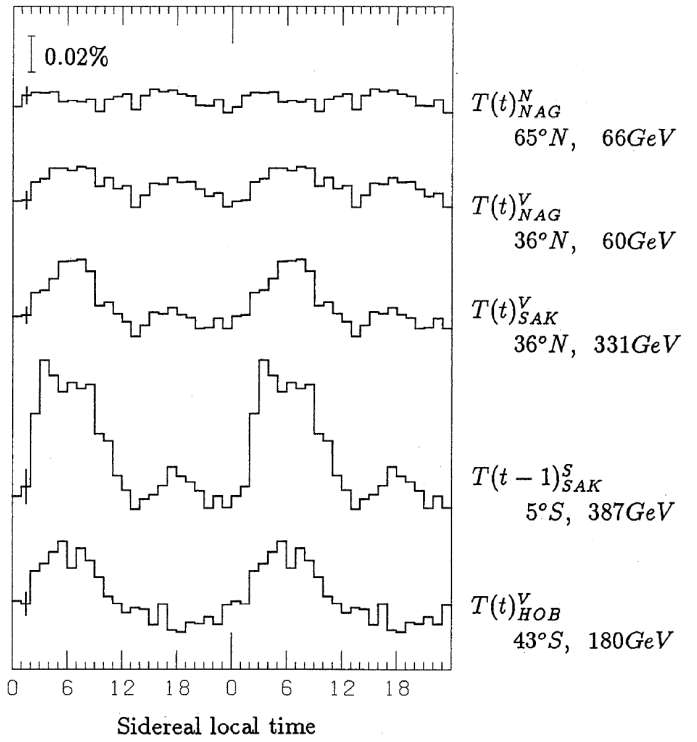

Fig. 16. $T(t_{S_i})$ due to TA obtained according to the preceding procedure shown in Fig. 15.

from the direction Φ_T ($\alpha_T \sim 6$ hr, $\delta_T \sim -24°$). Φ_T approximately coincides with the heliomagnetotail direction ($\alpha_{TP} = 6$ hr, $\delta_{TP} = -29.2°$) inferred from the direction of proper motion of the solar system (Campbell and Moore, 1928), although it is emphasized that this is different from the inferred tail direction ($\alpha_{TN} = 4.8$ hr, $\delta_{TN} = 15° \sim 17°$) opposite to the relative motion of the solar system to the neutral gas (Ajello, 1978; McClintock *et al.*, 1978). This difference will be discussed later.

The space distribution of TA is shown on the map in Fig. 18, together with that of GA (cf. Nagashima *et al.*, 1989). In Fig. 18, the excess cone of TA, within which all the directional excess flux is confined, is shown bounded by the thick line. A thinner line bounds the deficit cone of GA, in which all the directional deficit flux is confined. As can be seen in the figure, a telescope directed to the region of

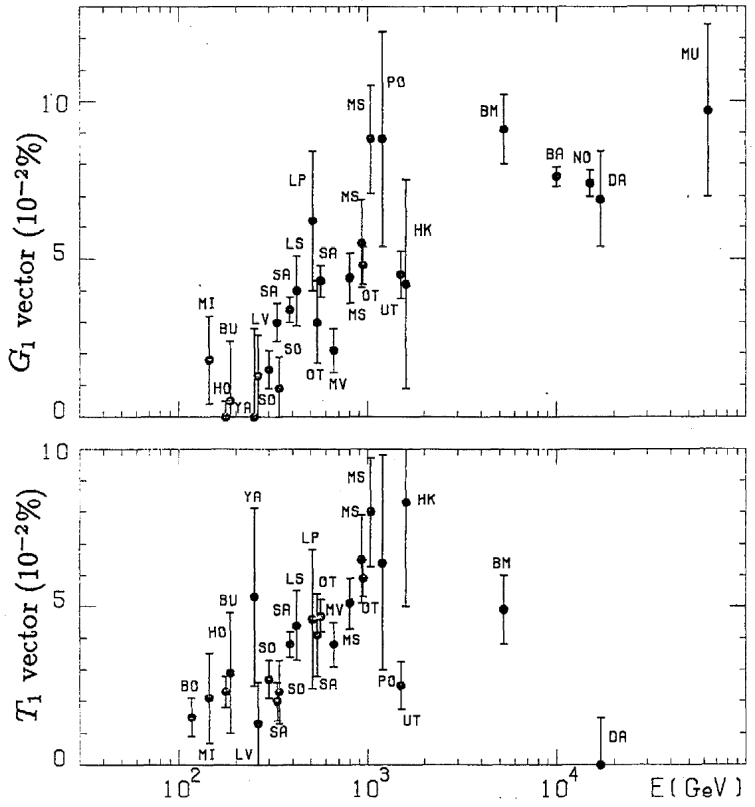

Fig. 17. Energy dependencies of the amplitude $\mathbf{GD_1}$ (0 hr) and $\mathbf{TD_1}$ (6 hr) derived from the observed $\mathbf{S_iD_1}$'s whose phases are shown in Fig. 12 (Ref. 3). The symbols are the same as in Fig. 12. The amplitude for $\lambda \neq 0°$ is converted into that at the equator by multiplying a provisional correction factor $1/\cos\lambda$, although its latitude dependence cannot be exactly expressed by $\cos\lambda$ as it contains the north-south asymmetric term ($\sin\lambda$).

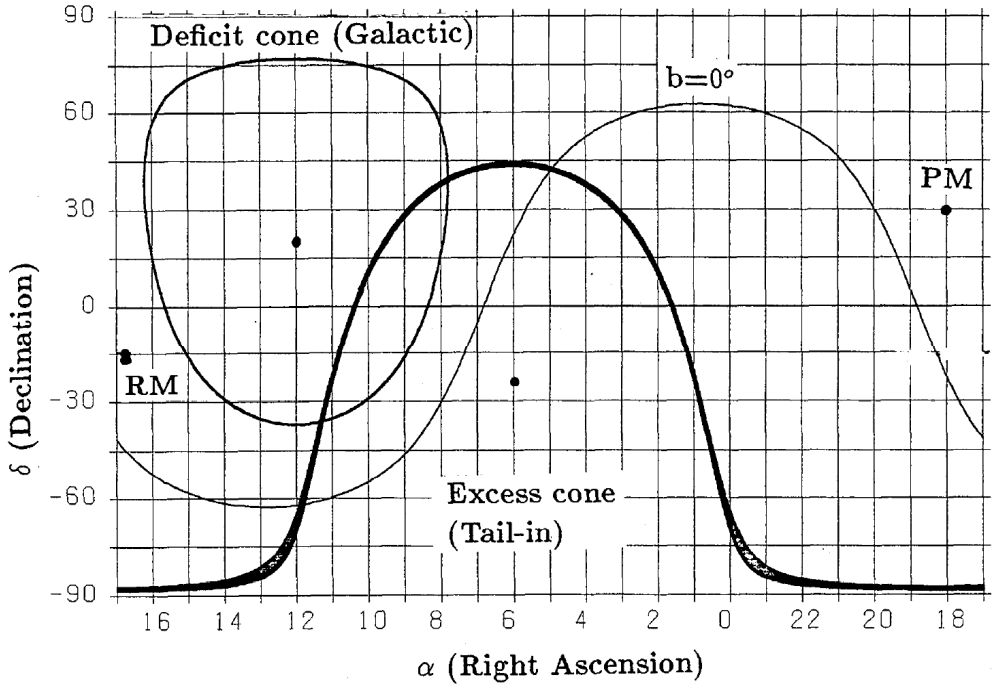

Fig. 18. The distribution of the tail-in (TA) and galactic (GA) anisotropies on the equatorial coordinate grid (Ref. 3). The excess cone of TA, within which all the directional excess flux is confined, is shown bounded by the thick line including the south pole. A thinner line bounds the deficit cone of GA, in which all the directional deficit flux is confined (cf. Nagashima *et al.*, 1989). PM, direction of proper motion of the solar system; RM, direction of relative motion of the system to the neutral gas; (thin line), galactic equator.

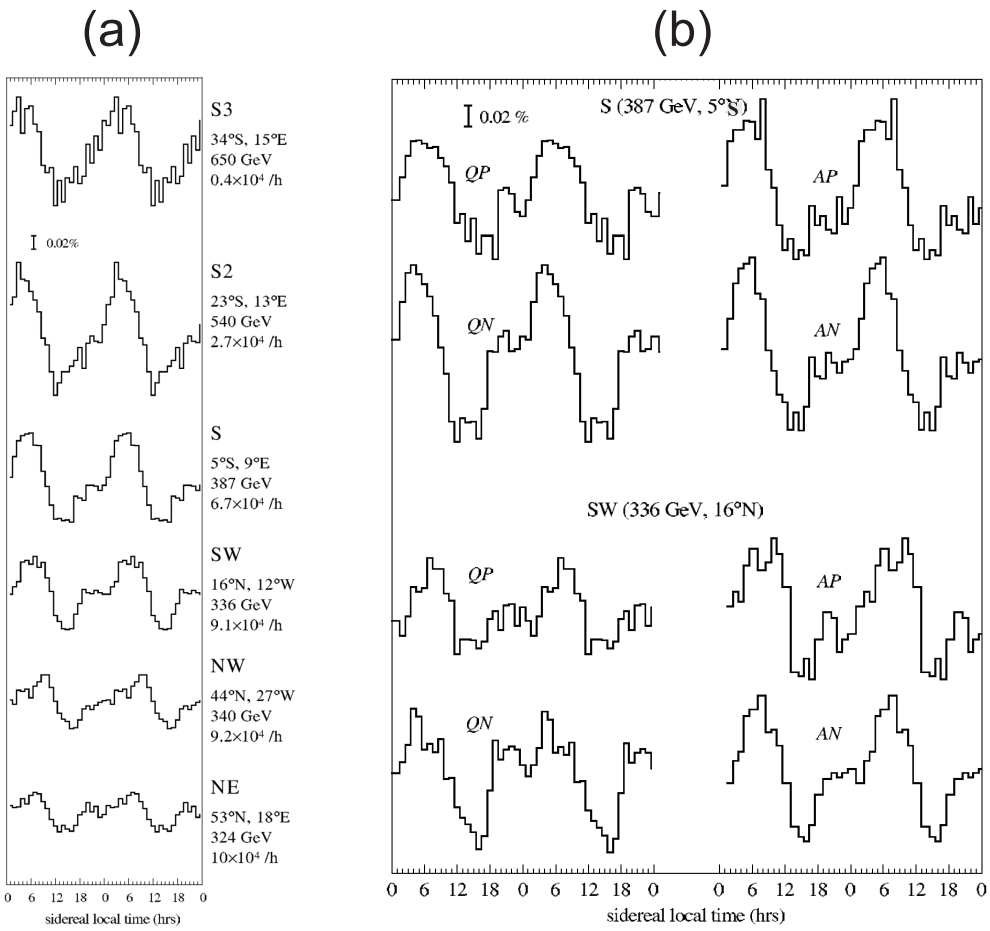

Fig. 19. Solar modulation of $G(t_{S_i})$ and $T(t_{S_i})$ observed by the underground muon telescopes (NE, NW, SW, $\cdots$ S3) at Sakashita in the period (1971–2000), (Nagashima *et al.*, 2004). (a) The latitude dependence of $G(t_{S_i})$ and $T(t_{S_i})$. (b) The polarity (P or N) and solar activity (A or Q) dependence of the two components 'SW' and 'S' in (a), which shows the most clear coexistence of $G(t_{S_i})$ and $T(t_{S_i})$, are separated, respectively, into four periods of AP, QP, AN and QN. The magnitudes of $G(t_{S_i})$ and $T(t_{S_i})$ show, respectively, the proper modulation patterns shown by Eqs. (1) and (2).

$\delta > \sim 44^\circ$ or $\delta < -37^\circ$ can observe only one of GA and TA as it sweeps either the deficit cone only, or the excess cone. In fact, the air shower observation ($E_m \sim 7 \times 10^4$ GeV) at Liawenee (42°S, 147°E; height = 1060 m), Tasmania, Australia and also the underground (depth $\sim$ 357 m.w.e.) at Poatina, Tasmania could not find $\mathbf{GD_1}$ (Fenton *et al.*, 1990, 1995). On the other hand, a telescope directed to the intermediate region of $\sim 44^\circ > \delta > -37^\circ$ successively sweeps the excess and deficit cones and would observe a complicated α-distribution of the variational intensity as shown in Fig. 14(a). It is easily understandable that such GA and TA can solve at least qualitatively all the previous problems except that of the absence of the polarity dependence at $\mathbf{S_iD_1}$ which will be resolved after the HMS modulation of GA and TA has been determined. It is further noted here that the discovery of GA and TA was soon supported by joint observations in the northern and southern hemispheres at Matsushiro (37°N), (cf. Mori *et al.*, 1981, 1989, 1993) and at Poatina (42°S), (Hall *et al.*, 1998, 1999).

5. Modulation of Anisotropies in the HMS

The HMS modulation of $G(t_{S_i})$ and $T(t_{S_i})$ shown in Fig. 19 has been obtained by the multi-directional muon telescopes at the underground station Sakashita (36°N, 138°E, 331 GeV), (Nagashima *et al.*, 2004; Ueno *et al.*, 1984). The latitude distribution of $S_iD(t_{S_i})$ in Fig. 19(a) indicates clearly the coexistence of $G(t_{S_i})$ and $T(t_{S_i})$. The peak at 6 hours expresses $T(t_{S_i})$ and the step-type variation on the left side of $T(t_{S_i})$ expresses a part of $G(t_{S_i})$. $T(t_{S_i})$ increases toward the southern hemisphere while the variation of $G(t_{S_i})$ is against $T(t_{S_i})$. The most typical coexistence of $T(t_{S_i})$ and $G(t_{S_i})$ is observed by the S- and SW-component telescopes. These variations are shown in Fig. 19(b) after being classified into four groups AP, AN, QP and QN in which P and N indicate P- and N-states, and A and Q are the Active and Quiet periods of solar activity. In the figure, $G(t_{S_i})$, which appears as a part of the plateau, has the following magnitude relation between four periods, which is called the modulation pattern hereafter.

$$G(t_{S_i}): \mathrm{QN} > \mathrm{AN} > \mathrm{QP} > \mathrm{AP}, \quad \text{for } 330 \sim 650 \text{ GeV}. \tag{1}$$

$G(t_{S_i})$ is larger in the Q-period than the A-period. This gives a firm basis on the galactic origin of $G(t_{S_i})$ as the galactic CR-flux suffers less disturbance in a Q-period than an A-period during its passage through the HMS, and is larger in the N-state than in the P-state. According to the modulation model (Refs. 1 and 2), this polarity dependence

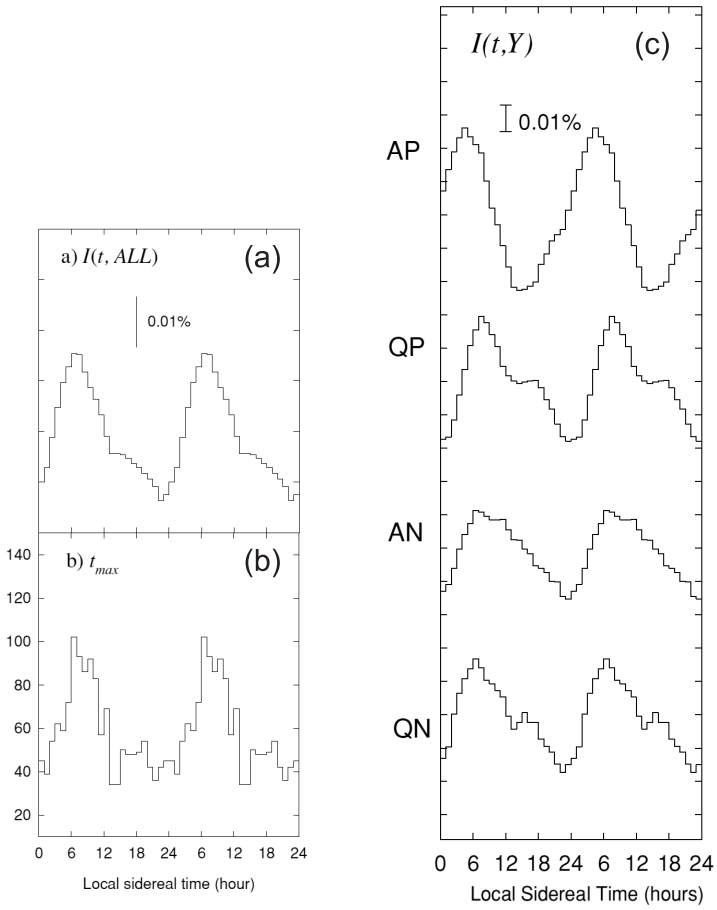

Fig. 20. (a) The average of yearly $S_iD(t_{S_i})$'s of neutron intensities observed at 74 stations in the period of 1960–2000. (b) Histogram of the maximum phase of yearly $S_iD(t_{S_i})$'s. (c) The modulation patterns of $S_iD(t_{S_i})$.

can be realized only when the direction of GA is near the equatorial plane of the HMS. This inferred direction is in good accord with that ($\delta_G = 20^\circ$) estimated from the space distribution of $G(t_{S_i})$ pointed out previously (cf. Fig. 18). On the contrary, $T(t_{S_i})$ with a sharp peak at ∼6 hours has a modulation pattern which is almost quite the opposite to that of $G(t_{S_i})$ as follows, (cf. Fig. 19).

$$T(t_{S_i}): \mathrm{QN} < \mathrm{AN} \sim \mathrm{QP} < \mathrm{AP}, \quad \text{for } 330 \sim 650\ \mathrm{GeV}. \tag{2}$$

$T(t_{S_i})$ is larger in an A-period than in a Q-period. This cannot be realized by the galactic anisotropy. The only possible solution is to assume the acceleration of galactic CRs proportional to the solar activity in the HMS. Furthermore, $T(t_{S_i})$ is larger in the P-state than the N-state, especially in the AP-period showing quite opposite polarity dependence to that of $G(t_{S_i})$ (cf. Fig. 19(b)). This would draw an inference for the location of the acceleration of CRs in the HMS, as will be discussed later together with other kinds of evidence. Whatever the mechanism of the origin of TA may be, however, it is clear that the modulation pattern in Eq. (2) is quite the reverse of that of GA in Eq. (1) as can be clearly seen in Fig. 19(b), and, as a result, the polarity-dependencies of GA and TA would always compensate each other. This would be the reason why the observation of the polarity dependence of $\mathbf{S_iD_1}$ did not show that expected from GA of the modulation model.

The existence of $T(t_{S_i})$ in the lower energy region was inferred from $\mathbf{TD_1}$ in Fig. 9 observed by neutron monitors (Nagashima *et al.*, 2005). In order to study the modulation pattern of $T(t_{S_i})$, $S_iD(t_{S_i})$'s were obtained by using neutron monitor data at 74 stations (WDC-C2 Center) in the period 1960–2000. Their average $\langle S_iD(t_{S_i})\rangle$ for all the stations, for all the years, was obtained by neglecting the difference of geomagnetic deflection angles at each station, as shown in Fig. 20(a). The histogram of the maximum phases (t_{max}) of the yearly-averaged first harmonic component $\mathbf{S_iD_1}$'s of $S_iD(t_{S_i})$ for all the stations during the entire period is shown in Fig. 20(b) (cf. Nagashima *et al.*, 2005). It is clear that the sharp peak of $S_iD(t_{S_i})$ at ∼6 hours exactly corresponds to the $T(t_{S_i})$. In addition, $S_iD(t_{S_i})$ contains another variation which is almost submerged beneath $T(t_{S_i})$ and can be narrowly recognized by the unnatural distribution in the time interval of $15 < t_{S_i} \leq 21$ hours (cf. Fig. 20(a)). This distribution is supposed to be produced by the superposition of the individual yearly harmonic components with their maximum in the above time interval ($15 < t_{S_i} \leq 21$ hr) as can be seen in the histogram in Fig. 20(b). The variation is a maximum at ∼18 hours and is called $H(t_{S_i})$ hereafter. The modulation pattern of $S_iD(t_{S_i})$ is shown in Fig. 20(c). $S_iD(t_{S_i})$ in the AP-period seems to be almost purely $T(t_{S_i})$ and the largest in all the periods, while others are supposed to become smaller by the interaction with $H(t_{S_i})$, as can be seen by the time shift of the minimum intensity from ∼12 hours

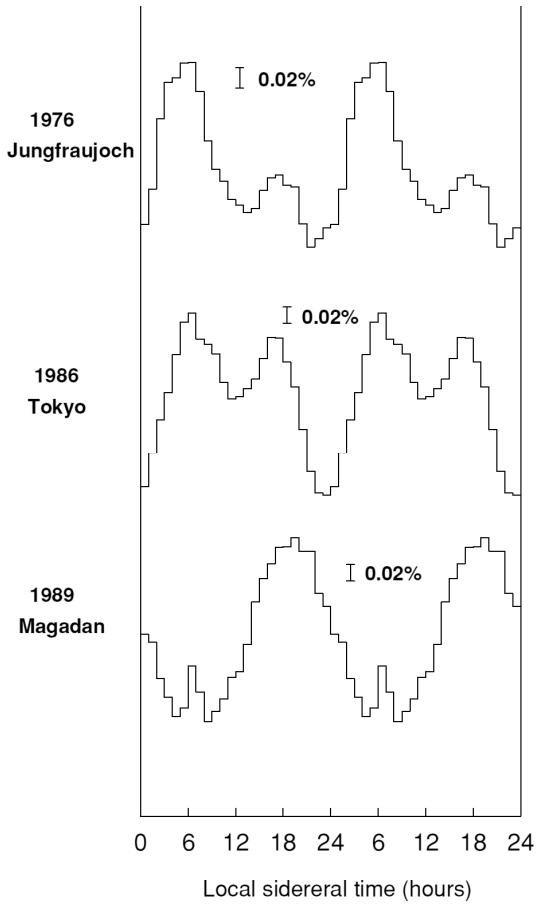

Fig. 21. Rise and fall of $T(t_{S_i})$ and $H(t_{S_i})$ of the neutron intensity with their maximum phases, respectively, at 6 hours and 18 hours, (Nagashima *et al.*, 2005).

to ∼24 hours and also by the appearance of smaller peaks in the QP- and QN-periods. $T(t_{S_i})$ has a modulation pattern nearly equal to that at the underground station Sakashita as

$$T(t_{S_i}) : \mathrm{QN} < \mathrm{AN} \leq \mathrm{QP} < \mathrm{AP}, \quad \text{for} \quad \sim 20\ \mathrm{GeV}. \tag{3}$$

The modulation pattern for $H(t_{S_i})$ cannot be obtained because of the lack of its explicit form in Fig. 20(c). $H(t_{S_i})$, however, can be clearly observed at some stations in some times together with $T(t_{S_i})$ as shown in Fig. 21. It has a sharp peak at ∼18 hours as expected and is called hereafter the nose-in anisotropy. $H(t_{S_i})$ and $T(t_{S_i})$ are unstable and easily reduce their magnitudes by their mutual interaction, resulting in the averaged small variations shown in Figs. 20 and 21.

Although $H(t_{S_i})$ was first found by neutron monitors, its separation from $T(t_{S_i})$ was more clearly seen in the muon telescopes at Nagoya (35°N; 137°E) as shown in Fig. 22(a) (Nagashima and Fujii, 2006). The variation with a large peak at ∼6 hours expresses $T(t_{S_i})$ and that of the small one with a maximum at ∼18 hours expresses $H(t_{S_i})$. Among them, the S-component (5°N, 64 GeV), which is characterized by the most remarkable $H(t_{S_i})$, is separated into the four groups as shown in Fig. 22(b). Their modulation patterns are

$$T(t_{S_i}) : \mathrm{QN} \sim \mathrm{AN} < \mathrm{QP} \ll \mathrm{AP}, \quad \text{for} \quad 60 \sim 100\ \mathrm{GeV}, \tag{4}$$

$$H(t_{S_i}) : \mathrm{QN} < \mathrm{AN} > \mathrm{QP} > \mathrm{AP}, \quad \text{for} \quad 60 \sim 100\ \mathrm{GeV}. \tag{5}$$

$T(t_{S_i})$ is larger in an A-period than in a Q-period, similarly to those in Eqs. (2) and (3), but, in the present case, it is extremely larger in an AP-period than in a QP-period. This is due to the following reason. As can be seen in Fig. 23, the yearly decomposed variations of $T(t_{S_i})$ in the respective AP- and QP-periods show quite different variations. In a QP-period, all the variations show one or two peaks at ∼6 and/or ∼18 hours which can be regarded as being due to $T(t_{S_i})$ and/or $H(t_{S_i})$. In the case of two peaks, the variations are generally small. This is partly due to the interaction between $T(t_{S_i})$ and $H(t_{S_i})$ with the mutually opposite maximum phases. On the other hand, almost all $S_iD(t_{S_i})$s in Fig. 23(a) show a large single peak of $T(t_{S_i})$ at ∼6 hours, indicating that an AP-period activates $T(t_{S_i})$ and/or inactivates $H(t_{S_i})$. On the other hand, $H(t_{S_i})$ in Fig. 22(b) shows the largest enhancement in an AN-period, being different from $G(t_{S_i})$ in a QN-period and from $T(t_{S_i})$ in an AP-period. These differences will give a hint as to the origin of the anisotropies.

Now, as for the direction of HA, the declination δ_H has been estimated to be in the range of $21^\circ \sim 41^\circ$ by an analysis of muon data (cf. Nagashima and Fujii, 2006). For reference, one set of data used for the estimation of δ_H is the $S_iD(t_{S_i})$'s in Fig. 24(a). $H(t_{S_i})$ in these $S_iD(t_{S_i})$'s first appears in the E-telescope in the equatorial region as a tiny protuberance at ∼18 hours, then gradually increases toward the northern regions and finally reaches its maximum at the W-component. The latitude distribution of the magnitude of $H(t_{S_i})$ is shown in Fig. 24(b). In this data, the maximum appears at $\delta_H \sim 40^\circ$.

It is emphasized here that $H(t_{S_i})$ seems to be the same as $C_g(t_{S_i})$ to be produced by the C-G effect by the motion of the HMS, as their phases are considered to be the same as each other (18 hr). But, they differ in the following points. First of all, $C_g(t_{S_i})$ is a broad sinusoidal diurnal variation with a declination distribution of $\cos\delta$-type and has a flat energy spectrum (Gleeson and Axford, 1967). On the other hand, $H(t_{S_i})$ shows the sharply-concentrated diurnal variation with an N-S asymmetric δ-distribution (cf. Fig. 24) and has a soft energy spectrum which almost disappears in the energy region ≥300 GeV (cf. Fig. 19). Furthermore, $H(t_{S_i})$ is greater in an AN-period than a QN-period (cf. Eq. (5)). This is against the galactic origin hypothesis as $C_g(t_{S_i})$ must be smaller in the A-period than the Q-period like the behavior of the modulation pattern of $G(t_{S_i})$, (cf. Eq. (1)). Therefore, the C-G effect of CRs cannot be observed in an energy region less than 10^4 GeV, as pointed out previously (Ref. 3).

Finally, in addition to $T(t_{S_i})$ and $H(t_{S_i})$, Fig. 22(b) contains also $G(t_{S_i})$. $S_iD(t_{S_i})$ in a QN-period in the figure shows a straight line with its center at 0 hr and with the level higher than the lowest value at 12 hr. This line, called a g-line, is supposed to express a part of $G(t_{S_i})$ whose whole figure would be a trapezium bounded by the line through the fol-

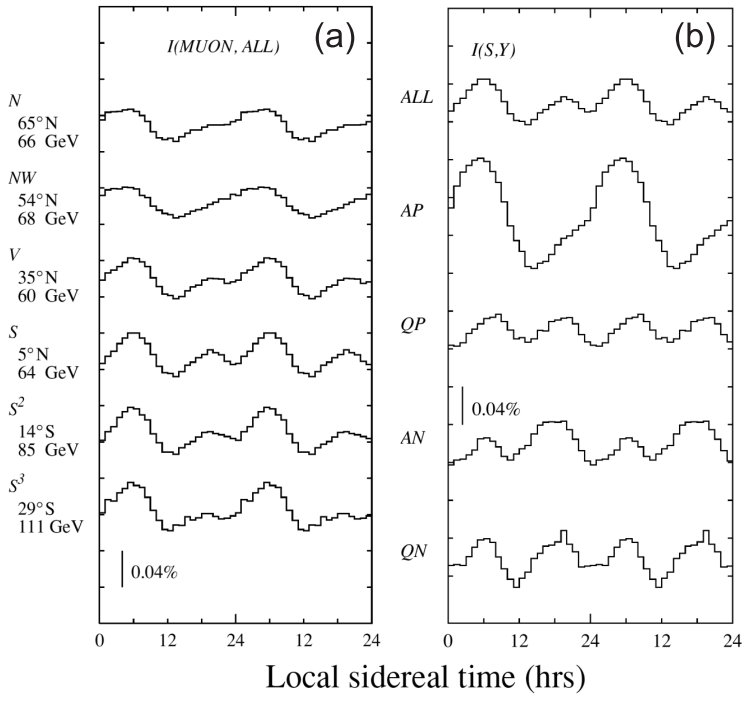

Fig. 22. (a) Latitude dependence of $S_iD(ts_i)$ observed by muon telescopes (S^3, S^2, S, $\cdots$ N) at Nagoya in the period of 1971–2003 to show the existence of $H(ts_i)$ with the maximum phase at 18 hr, and (b) the modulation pattern of $S_iD(ts_i)$ of S-component in (a) which shows clearly the existence of HA, (Nagashima and Fujii, 2006).

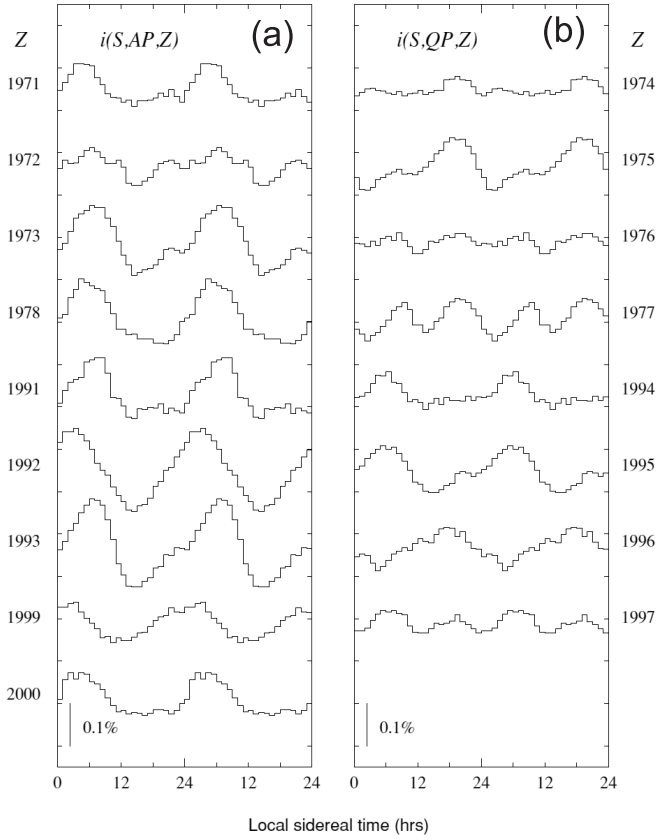

Fig. 23. Yearly variations of $S_iD(ts_i)$ in (a) AP and (b) QP periods in Fig. 22(b), showing the enhancement of $T(ts_i)$ in the AP-period due to less influence of $H(ts_i)$ at $ts_i = 18$ hr.

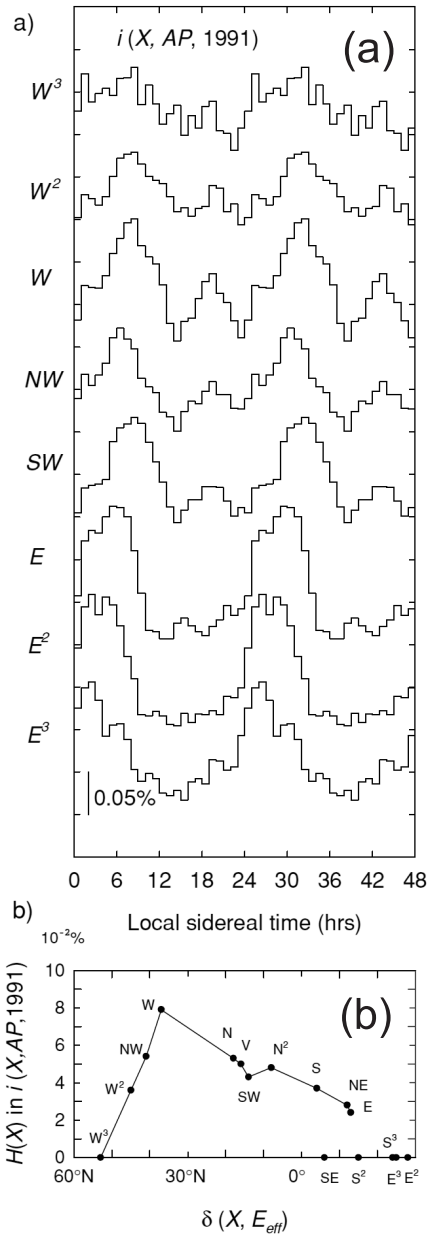

Fig. 24. (a) The rise and fall of $H(ts_i)$ with its maximum at 18 hr, and (b) the rigidity dependence of the magnitude of $H(ts_i)$, (Nagashima and Fujii, 2006).

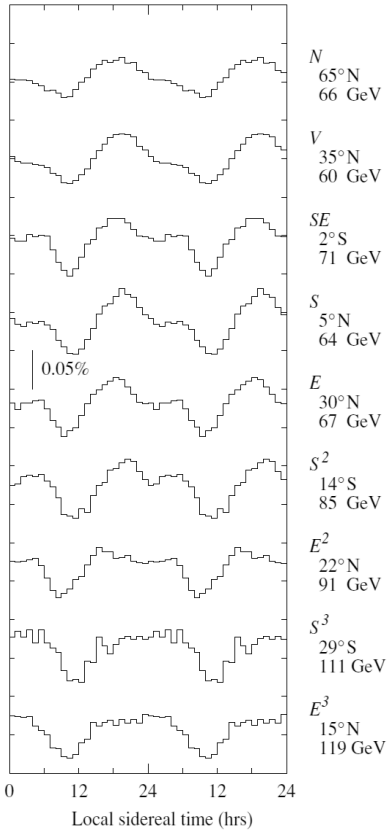

Fig. 25. The averages of $S_iD(ts_i)$'s for 6 years (1981, '83, '84, '87, '88, '89) in AN and QN periods, selected from those in Fig. 22(a). $G(ts_i)$ can be clearly seen, especially in the low latitude region.

lowing four points; g_1 and g_2 are the intersection points between the g-line and $S_iD(ts_i)$ near the 12 hours, and b_1 and b_2 are minimum points of $S_iD(ts_i)$ at 12 hours. Such a flat g-line disappears in AN, QP and AP-periods, but the influence of $G(ts_i)$ in a QN-period remains as a small dip at ∼0 hrs in the variation averaged for all the periods. The whole picture of the $G(ts_i)$'s can be seen in Fig. 25 which shows the averages of six selected years in AN- and QN-periods. $G(ts_i)$ appears as a typical plateau-type variation with a minimum at ∼12 hours in the equatorial regions and decreases towards the northern latitude with the gradual increase of $H(ts_i)$ with a maximum at 18 hours. It is noteworthy that similar enhancements of $G(ts_i)$ in the N-state have been observed also by the ion-chambers at Godhaven (69°N, 53°W; 67 GeV; 1936–1959; Lange and Forbush, 1948, 1957) and at Yakutsk (62°N, 130°E; 67 GeV; 1953–1980; Shafer and Shafer, 1984), (cf. Nagashima and Fujii, 2006).

6. Origin of GA, TA and HA, and the Related Discussion

6.1 Origin of GA, TA and HA

The three anisotropies GA, TA and HA mentioned earlier are subjected, respectively, to different modulation patterns as shown in Eqs. (1)–(5) and in Table 1. The patterns clearly indicate that GA could be explained at least qualitatively by a dependence on the polarity state and on the solar activity expected from the modulation model (Refs. 1 and 2) and that it arrives from galactic space near the equatorial plane of the HMS ($\delta \sim 0°$), which is in good agreement with the direction Φ_G ($\alpha_G = 0$ hr and $\delta_G = -24°$) shown in Fig. 18. On the other hand, TA and HA are supposed to be of a non-galactic origin as they produce, respectively, larger variations $T(ts_i)$ and $H(ts_i)$ in the A-period than in the Q-period. The most plausible source of TA and HA would be the acceleration of galactic cosmic rays on the HMS boundary with the nose and tail, being composed of the aggregation of point sources with their main axes perpendicular to the boundary surface. As TA and HA are produced by a curved surface source, unlike the plane source of GA, the modulation model for GA cannot be applied to TA and HA. However, the CRs in the HMS which can arrive at the Earth from the high latitude boundary ($|\lambda| \gg 0°$) in the P-state, and from the equatorial region ($\lambda \sim 0°$) in the N-state, do

Table 1. Modulation pattern of sidereal anisotropy by GA, TA, and HA.

	Polarity 22 yr period P N	Solar activity 11 yr period A Q	Direction Φ α (hr)	δ(°)	Origin
GA	<	<	0	−20	Galactic
TA	>	>	6	−24	Solar (Tail boundary)
HA	<	>	18	>0	Solar (Nose boundary)

not drastically change their behavior in spite of the deformation from the spherical boundary to a comet-like structure. This behavior can explain the modulation patterns of $T(t_{S_i})$ and $H(t_{S_i})$ assuming that:

(1) The structure of the HMS is surrounded by the nose- and tail-boundaries, and has a wavy neutral sheet at the heliomagnetic (HM) equatorial plane which divides the HM polarity states in the N- and S-hemispheres.
(2) CRs are assumed to be accelerated uniformly all over the boundaries depending on the solar activity.

The polarity dependence of $T(t_{S_i})$ that is,

$$|T(t_{S_i})|_P > |T(t_{S_i})|_N \tag{6}$$

would be produced by the following process. The accelerations of CRs responsible for $|T(t_{S_i})|_P$ are limited on the northern-most and southern-most narrow tail boundary regions. In the P-state, all the CRs having been ejected from the specified region in the above are deflected towards the Sun. If the source region is far away from the Sun, some selected CRs could arrive at the Earth through the wavy neutral sheet and others would escape from the HMS through the northern and southern boundaries (cf. Fig. 26). Such northern- and southern-most regions are called R_b hereafter. The flux of TA responsible for $T(t_{S_i})$ is the congress of those selected CRs. The sharply-concentrated distribution from the direction of $\alpha = 6$ hr would be determined by two factors: the width of the narrow boundary region, and the amplitude of the wavy neutral sheet. For the transition from the P-state to the N-state, the CRs ejected from the boundaries change their direction towards the tail-end side and cannot be observed at the Earth. Instead, alternative flux from the area (S_{te}) of the tail-end near the central line of the neutral sheet can arrive at the Earth along the wavy neutral sheet after automatically forming the sharply concentrated flux (TA) from the direction of $\alpha = 6$ hr, similar to the distribution in the P-state. In this case, some additional contribution to the flux might be expected from the two side-boundaries of the tail near the sheet. But this contribution is likely to be negligible, as almost all the CRs from the side-boundaries far away from the Sun escape from the HMS across the other side-boundary without changing their direction. Such a process to formulate the sharply-concentrated flux from $\alpha = 6$ hr is called hereafter the CR Lens Effect by the HMS.

The polarity dependence of Eq. (6) can be realized if the HMS tail is extended long enough to achieve the CR flux from the total sum of R_b larger than that of the tail-end region (R_e) near the central line of the neutral sheet.

On the other hand, the polarity dependence of $H(t_{S_i})$ shown by Eq. (7) is observed in the head-side region of the HMS where the CR trajectories are given by the axis-symmetric reversal of those in Fig. 26 with respect to the solar magnetic polar axis.

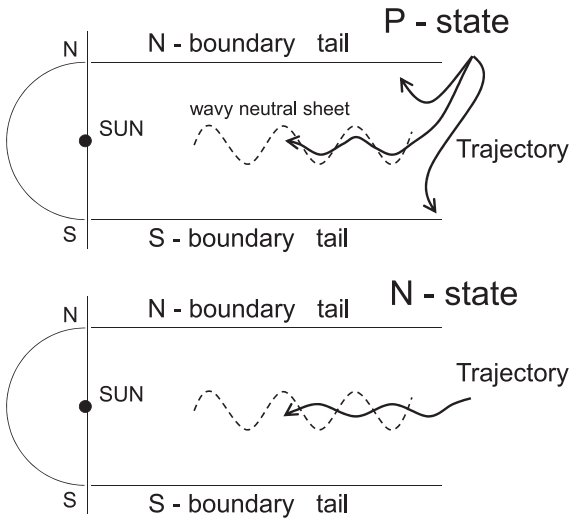

Fig. 26. Cosmic-Ray-Lens Effect of HMS which focuses CRs along the direction of the neutral sheet of HMS. Arrowed curves express the CR trajectories in P- and N-states. Dashed line is the wavy neutral sheet.

$$|H(t_{S_i})|_P < |H(t_{S_i})|_N. \tag{7}$$

As the movement of CRs in the region is the same as before, all the statements in the case of TA are applicable also in the present case. Therefore, the polarity dependence in Eq. (7) can be satisfied if the nose-boundary length is shortened so that the CR flux from the total sum of R_b becomes smaller than that from the head region (R_h) near the central line of the neutral sheet. It is emphasized here that the direction of motion of the HMS in space, in other words the direction of the nose and tail of the HMS, can be determined automatically by the HMS modulation of HA and TA without any aids, such as the motion of the HMS relative to the neighboring stars (Campbell and Moore, 1928).

6.2 Direction of nose head of the HMS in space

The nose direction (Φ_{HMS}) of the HMS can be determined by observation on the basis of the model. As pointed out earlier, the T- and H-anisotropies are observed in the respective directions Φ_T ($\alpha_T = 6$ hr, $\delta_T = -24°$) and Φ_H ($\alpha_H = 18$ hr, $\delta_H = 24° \sim 41°$), both of which could be considered to constitute a straight line through the Sun; that is, the center line of the neutral sheet of the HMS. Therefore, the motion of the HMS would be in the direction Φ_{HMS} ($\alpha_{HMS} = 18$ hr, $\delta_{HMS} = 24°$) and should produce the C-G effect of CRs from the direction of 18 hr. Contrary to this expectation, the C-G effect could not be observed

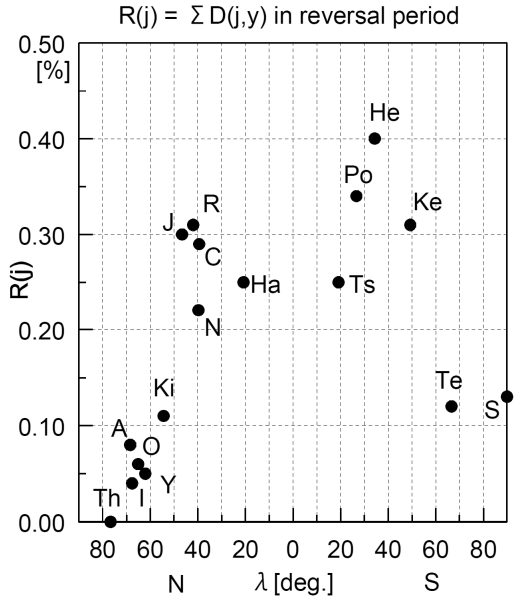

Fig. 27. The latitude distribution of the magnitudes R(j)'s of the total sum of D(j, y)'s in the respective reversal periods, where D(j, y) shows the monthly vector $\mathbf{S_oD_1}$ of neutrons in the text whose phase is toward the night sides in 1995–1996. P: south pole, Te: Terre Adelie, Ke: Kerguelen, He: Hermanus, P: Potchefstroom, Ts: Tsumeb, Ha: Haleakala, C: Climax, N: Newark, R: Rome, J: Jungfraujoch, Ki: Kiel, Y: Yakutsk, O: Oule, A: Apatity, I: Inuvik, Th: Thule (Nagashima *et al.*, 2010).

(Nagashima *et al.*, 1998). The non-existence of the effect is of importance with regard to the interaction between the HMS and the interstellar gaseous matter (IGM), as will be discussed in the next section.

The motion of the HMS is further supported by the seasonal variation of T(t_{S_i}) which shows the maximum flux at the December solstice as pointed out earlier (cf. Fig. 13). This flux produces the maximum T(t_{S_i}) with the phase of $\alpha_T = 6$ hr and can also be observed on the Earth as the solar diurnal variation $\mathbf{S_oD_1^T}$ with the maximum phase at 0 hr local solar time (t_{S_o}) at the December solstice ($\alpha_T = 6$ hr). This phase ($t_{S_o} = 0$ hr) is opposite to the daytime phase of $\mathbf{S_oD_1}$ due to S_oA caused by the CR diffusion convection in interplanetary space (Gleeson and Axford, 1967; Munakata and Nagashima, 1986). If $\mathbf{S_oD_1^T}$ is larger than $\mathbf{S_oD_1}$, the observed phase will be reversed towards the night side, suggesting the existence of the seasonal variation of T-anisotropy. The reversal has happened during several months of the winter season around the December solstice in the solar activity minimum period (1995/96) in the P-state when the enhancement of TA and the depressions of GA and S_oA were observed (cf. Table 1). The magnitude of the reversal, and its duration periods, depend on the latitude of the stations. The total magnitude of the reversals at each neutron monitor station in Fig. 27 shows a clear north-south asymmetry with the maximum in the southern hemisphere, which means that the declination (δ_T) of the T-anisotropy is negative; in other words, that (δ_{HT}) of the nose direction (Φ_{HT}) is positive (Nagashima *et al.*, 2010). It is further noted that the reversal has been observed in the period by the muon telescopes (60 GeV) at Nagoya (cf. Nagashima *et al.*, 2010).

6.3 The duality of the motion of solar system in space

As above, the direction of the motion ($\mathbf{V^C_{HMS}}$) of the solar system inferred from the HMS modulation of the TA and HA is Φ^C_{HMS} ($\alpha_{HMS} = 18$ hr; $\delta_{HMS} = 24^\circ$) and coincides with Φ^S_{HMS} of the motion of the HMS relative to the neighboring stars (Ajello, 1978; McClintock *et al.*, 1978), (cf. Table 2). On the other hand, the corresponding direction of the motion ($\mathbf{V_{np}}$) of the HMS relative to neutral particles observed by the space probe is Φ_{np} ($\alpha_{np} = 16.2$ hr; $\delta_{np} = -15^\circ \sim -17^\circ$) and clearly different from Φ^C_{HMS}. The difference is likely to be attributable to the inaccurate observation by the CR charged particles, because the motion of the neutral and ionized gases in space would have been in an equilibrium state by their mutual interaction over the long-term in the past, and also the motion of the neutral gas is supposed to be more easily observable without any influence of interstellar- and helio-magnetic fields. The judgement on this matter seems to be correct in so far as one adheres to the conventional C-G effect for the relative motion of the HMS to the ionized and neutral particles moving freely in space. The physical state of the interstellar space, however, is supposed to be different from this assumption and the interstellar gaseous matter (IGM) containing the ionized and neutral particles, together with the magnetic field ($\mathbf{B_{ISM}}$), is supposed to be a good electromagnetic conductor and moving itself in some direction in space. It will be shown in the following that this assumption explains the duality of $\mathbf{V^C_{HMS}}$ and $\mathbf{V_{np}}$ observed, respectively, by the CRs and the neutral particles.

As pointed out previously, the direction Φ^C_{HMS} of the motion ($\mathbf{V^C_{HMS}}$) of the HMS inferred from the sidereal diurnal variation of CRs almost exactly coincides with that (Φ^S_{HMS}) of the motion ($\mathbf{V^S_{HMS}}$) of the HMS relative to the neighboring stars and, therefore, $\mathbf{V^C_{HMS}}$ is renamed $\mathbf{V^{CS}_{HMS}}$ for convenience (cf. Table 2). This coincidence indicates that $\mathbf{V_{np}}$ is not due to the motion of the HMS itself, but due to the flow $\mathbf{V^{HMS}_{np}}$ of the neutral particles relative to the HMS with the phase Φ^{HMS}_{np} ($\alpha^{HMS}_{np} = 4.2$ hr; $\delta^{HMS}_{np} = 15^\circ \sim 17^\circ$). $\mathbf{V^{CS}_{HMS}}$ and $\mathbf{V^{HMS}_{np}}$ are coplanar as shown in Fig. 28. Their relative configuration is obtained in polar coordinates (r, δ, ϕ) on the assumption that $\mathbf{V^{CS}_{HMS}}$ is nearly equal to $\mathbf{V^S_{HMS}}$ (cf. Table 2). $\mathbf{V^{CS}_{HMS}}$ expresses the motion of the HMS relative to the neighboring stars, while $\mathbf{V^{HMS}_{np}}$ is relative to the HMS and can be transformed to a new vector $\mathbf{V^S_{IGM}}$ relative to the stars, as shown in Fig. 28. $\mathbf{V^S_{IGM}}$ expresses the motion of the interstellar gaseous matter (IGM) relative to the stars and $\mathbf{V^{HMS}_{np}}$ is interpreted as the transformed $\mathbf{V^S_{IGM}}$ observed on the moving frame ($\mathbf{V^{CS}_{HMS}}$) of the HMS. $\mathbf{V^S_{IGM}}$ is determined in the polar coordinates (r, δ, α) as shown in Table 2, and the relative configuration among $\mathbf{V^S_{IGM}}$, $\mathbf{V^{CS}_{HMS}}$ and $\mathbf{V^{HMS}_{np}}$ are specified as shown in Fig. 28. As the IGM is electromagnetically a good conductor, it would interact with the HMS. The magnetic field $\mathbf{B_{IGM}}$ in IGM would be pushed or dragged by the HMS and would be strengthened and forced to move with the HMS. In addition to this interaction, there is another interaction of the HMS with IGM which is moving vertically towards the southern hemispherical boundary of the HMS (cf. Fig. 28). However, their direct interaction would be reduced as IGM gradually changes

Table 2.

	V (km/s)	α (hr)	δ (°)
$\mathbf{V}^{\mathbf{S}}_{\mathbf{HMS}}$ of HMS relative to Stars	19.65	18.04	29.2
$\mathbf{V}^{\mathbf{C}}_{\mathbf{HMS}}$ of HMS observed by CRs		18	24
$\mathbf{V}^{\mathbf{CS}}_{\mathbf{HMS}}$ of HMS relative to Stars	(∼20)	18	24
$\mathbf{V}_{\mathbf{np}}$ between np and HMS		16.8	$-15 \sim -17$
$\mathbf{V}^{\mathbf{HMS}}_{\mathbf{np}}$ of np relative to HMS	26	4.8	$15 \sim 17$
$\mathbf{V}^{\mathbf{S}}_{\mathbf{IGM}}$ of IGM relative to Stars	17.5	0	66.5

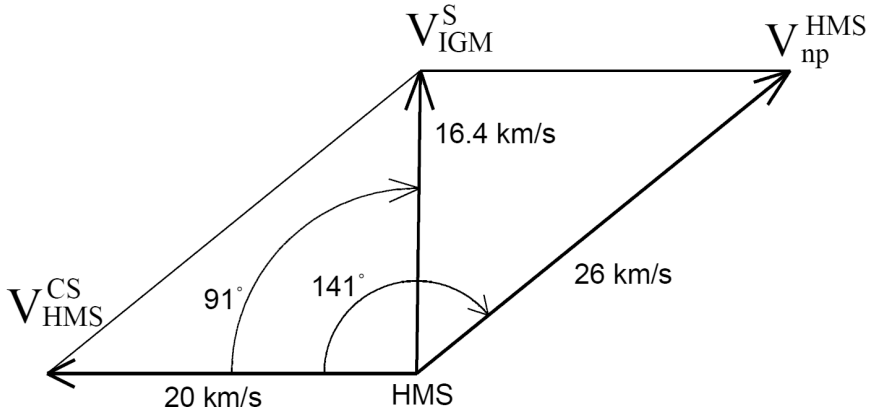

Fig. 28. Motion $\mathbf{V}^{\mathbf{S}}_{\mathbf{IGM}}$ of the interstellar gaseous matter (IGM) relative to the neighboring stars (S) inferred from the motion $\mathbf{V}^{\mathbf{CS}}_{\mathbf{HMS}}$ of HMS relative to S observed by CRs and the motion $\mathbf{V}^{\mathbf{HMS}}_{\mathbf{np}}$ of the neutral particles (np) relative to the HMS.

its direction toward $\mathbf{V}^{\mathbf{CS}}_{\mathbf{HMS}}$ with the approach to the HMS by the dragging effect of the HMS. Therefore, the interaction region remains almost axis-symmetrically with respect to the direction of $\mathbf{V}^{\mathbf{CS}}_{\mathbf{HMS}}$. Such an interaction region surrounding the whole HMS is called hereafter the Subordinate HMS (S_uHMS) of the HMS, whose outer boundary becomes beyond recognition as the magnetic field ($\mathbf{B_{SuH}}$) inside the S_uHMS gradually reduces its strength toward the outside and tends to $\mathbf{B_{IGM}}$ at the boundary. It is noted that the present interaction cannot produce the so-called bow shock in front of the HMS contrary to the prediction by Venkatesan and Badruddin (1990), because IGM has no velocity component of $\mathbf{V}^{\mathbf{S}}_{\mathbf{IGM}}$ parallel to $\mathbf{V}^{\mathbf{CS}}_{\mathbf{HMS}}$ (cf. Fig. 28) and is only passively pushed and/or dragged by the HMS. The S_uHMS could play a buffer role to reduce the direct interaction between the interstellar CRs and the HMS, if its width is larger than the gyration radius of CRs. Therefore, CRs with low energies confined in a stationary state in IGM would lose their ability to produce the C-G effect against the HMS by an interaction with the S_uHMS, showing good agreement with the undetectable C-G effect by CRs. Such a low-energy region would be extended at least up to $\sim 10^4$ GeV as the C-G effect could not be found by the air showers at Mt. Norikura (cf. Ref. 3). In high-energy regions, however, the C-G effect could be expected to be observed by the motion $\mathbf{V}^{\mathbf{CS}}_{\mathbf{HMS}}$ with 20 km/s (not $\mathbf{V_{np}}$) according to the process of the conventional C-G effect, as CRs could arrive at the HMS without any influence of $\mathbf{B_{IGM}}$ and $\mathbf{B_{SuH}}$.

On the other hand, the neutral particles in the IGM could not recognize the existence of the S_uHMS owing to their long scattering mean free path in comparison with the scale of the S_uHMS. Therefore, the particles are able to freely pass through the S_uHMS and the HMS with the velocity $\mathbf{V}^{\mathbf{S}}_{\mathbf{IGM}}$ and produce the motion $\mathbf{V}^{\mathbf{HMS}}_{\mathbf{np}}$ observed in the solar system (cf. Fig. 28).

As above, the introduction of the two proper motions $\mathbf{V}^{\mathbf{CS}}_{\mathbf{HMS}}$ and $\mathbf{V}^{\mathbf{S}}_{\mathbf{IGM}}$ relative to the neighboring stars could explain the duality of the motion of the HMS in space and prove also the absence of the C-G effect of CRs at low energies due to the motion of the HMS by the interaction of the S_uHMS surrounding the HMS. Furthermore, the interaction of the S_uHMS with the HMS can contribute to the acceleration of CRs at the boundary of the HMS required for the origin of TA and HA.

Finally, it is noteworthy that the existence of the motion of IGM relative to the neighboring stars has been found by the duality of the motion of the solar system in space probably for the first time.

6.4 Influence of TA and HA on S_oA

As pointed out previously, the seasonal variation of $\mathbf{TD_1}$ produces two sideband variations $\mathbf{S_oD_1^T}$ and $\mathbf{ES_iD_1^T}$ (cf. Fig. 13). $\mathbf{ES_iD_1^T}$ was found by the observation at Hobart and has contributed to the discovery of GA and TA. The other sideband variation $\mathbf{S_oD_1^T}$ with the phase 0 hr local solar time cannot be observed by the disturbance of $\mathbf{S_oD_1}$ of the solar origin due to the diffusion convection of CRs inside the HMS (cf. Gleeson and Axford, 1967), but can be estimated from $\mathbf{ES_iD_1^T}$ by the Farley-Storey method (cf. Fig. 2), and eliminated from the solar diurnal variation $\mathbf{S_oD_1^r}$ ($= \mathbf{S_oD_1} + \mathbf{S_oD_1^T}$). As another method, the influence of $\mathbf{S_oD_1^T}$ on $\mathbf{S_oD_1}$ can be directly observed by the relative configuration of $\mathbf{S_oD_1^T}$ to $\mathbf{S_oD_1}(j)$ and $\mathbf{S_oD_1^r}(j)$ at $j = X, Y$ and Z stations as shown on the solar diurnal harmonic coordinates in Fig. 29. In the figure, $\mathbf{S_oD_1^T}$, being assumed to

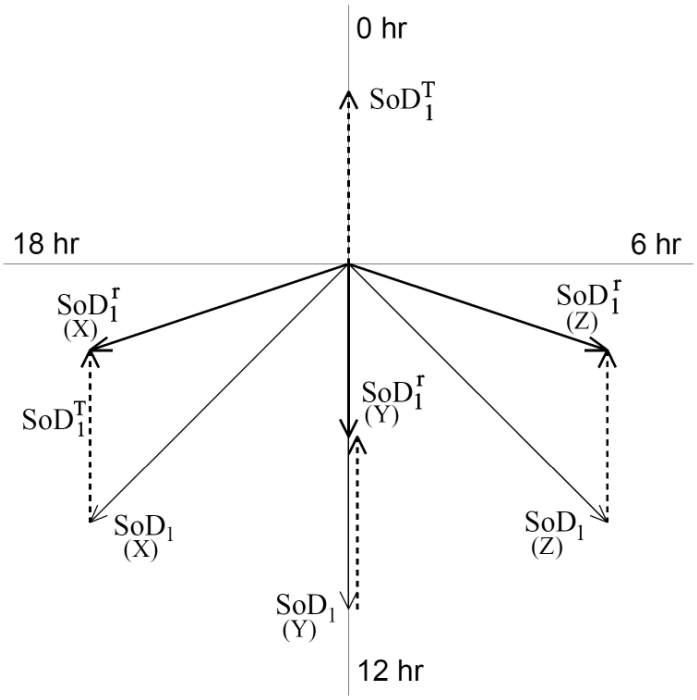

Fig. 29. Influence of three kinds of $\mathbf{S_oD_1}$ (X, Y and Z) caused by the seasonal variation $\mathbf{S_oD_1^T}$ of TA. $\mathbf{S_oD_1^r} = \mathbf{S_oD_1} + \mathbf{S_oD_1^T}$.

be constant at 0 hours by neglecting the geomagnetic deflection for simplicity, shortens all the vectors $\mathbf{S_oD_1}(j)$s and advances or retards their phases $\phi(j)$s in the 3rd or 2nd quadrant. However, $\mathbf{S_oD^r}(j)$ might be produced by a change of the direction Φ_{S_oA} and of the rigidity spectrum $f(p)dp$ of S_oA defined by

$$\begin{aligned} f(p)dp &= f_0 p^{\gamma} dp \quad \text{for } p \le p_u, \\ &= 0 \qquad\quad \text{for } p > p_u, \end{aligned} \tag{8}$$

where the exponent γ and the upper cut-off rigidity p_u are parameters. Under such circumstances, the existence of $\mathbf{S_oD_1^T}$ will be shown by the following process. Among the three unknown parameters Φ_{S_oA}, γ and p_u of S_oA, Φ_{S_oA} can be substituted by ϕ(INU) of $\mathbf{S_oD_1}$(INU) observed at the INUVIK station ($\lambda = 68^\circ$N, $\varphi = 226^\circ$E) as follows,

$$\Phi_{S_oA}(\gamma, p_u) = \phi(\text{INU} \mid \gamma, p_u) + \sim 9^\circ, \tag{9}$$

as the longitudinal geomagnetic deflection angles of CRs at the station are independent of p and given by $\sim -9^\circ$ (cf. Inoue *et al.*, 1983). Therefore, γ and p_u can be determined by the relative positions between $\mathbf{S_oD_1}(j)$ and $\mathbf{S_oD_1}$(INU) on the harmonic dial; in other words, by the following two quantities:

$$\mathrm{R}(j) = |\mathbf{S_oD_1}(j)|/|\mathbf{S_oD_1}(\text{INU})|,$$

and

$$\Delta\phi(j) = \phi(j) - \phi(\text{INU}). \tag{10}$$

These observed quantities can be compared respectively with the theoretical values obtained for various γ and p_u (cf. Yasue *et al.*, 1982; Fujimoto *et al.*, 1984). Figure 30 shows the R-$\Delta\phi$ diagram in which the theoretical R and $\Delta\phi$ are drawn as a function of γ and p_u by the net area. If the observed point is inside the area, $\mathbf{S_oD_1}(j)$ can be explained by S_oA with Φ_{S_oA}, γ and p_u at the point. The diagram on the left side of Fig. 30 is the distribution at the neutron monitor station Hermanus (3.4°S, 19°E; cut-off rigidity $p_c = 4.9$ GV) during the period (1965–2000), and on the right that at the muon station at Nagoya (35°N, 137°E; $p_c = 11.5$ GV). The number attached to each point expresses the observation year in the '70s and '90s in the P-state. As Φ_{S_oA} is dependent on the polarity and solar activity, showing near ∼18 hours in the AN-period and ∼15 hours in the QP-period, $\phi(j)$ also shows the same dependence (cf. Munakata and Nagashima, 1986). As $\mathbf{S_oD_1}$(Hermanus) and $\mathbf{S_oD_1}$(Tokyo) in the above vary their phases, respectively, from about 18 hr to ∼12 hr and ∼12 hr to the morning side by the dependence, they are typical examples for $j = X$ and Z in Fig. 29. $\mathbf{S_oD_1^r}$ (Nagoya) of the Z-type is converted into the right outside point of the net area on the R-$\Delta\phi$ diagram in Fig. 30. Almost all the points in the P-state deviate from the net area and the deviation increases with the decrease of solar activity and becomes a maximum in the solar activity minimum period (1976, '77, '96 and '97). Some of these points would be able to be included in an enlarged net area by increasing γ and reducing p_u, but it is very difficult to do so as such a large γ and small p_u cannot be accepted by the other analyses of the solar diurnal variation (cf. Nagashima *et al.*, 2010). The points in the N-state, on the other hand, are almost on the net area. Therefore, the influence of $\mathbf{S_oD_1^T}$ on $\mathbf{S_oD_1}$ cannot be confirmed, except for the following three points in the minimum period of solar activity (1986, '87 and '88), which show very small R's, being isolated from the other group (cf. Fig. 30). These points would be due to the influences of $\mathbf{S_oD_1^T}$ as $\phi(j)$ in

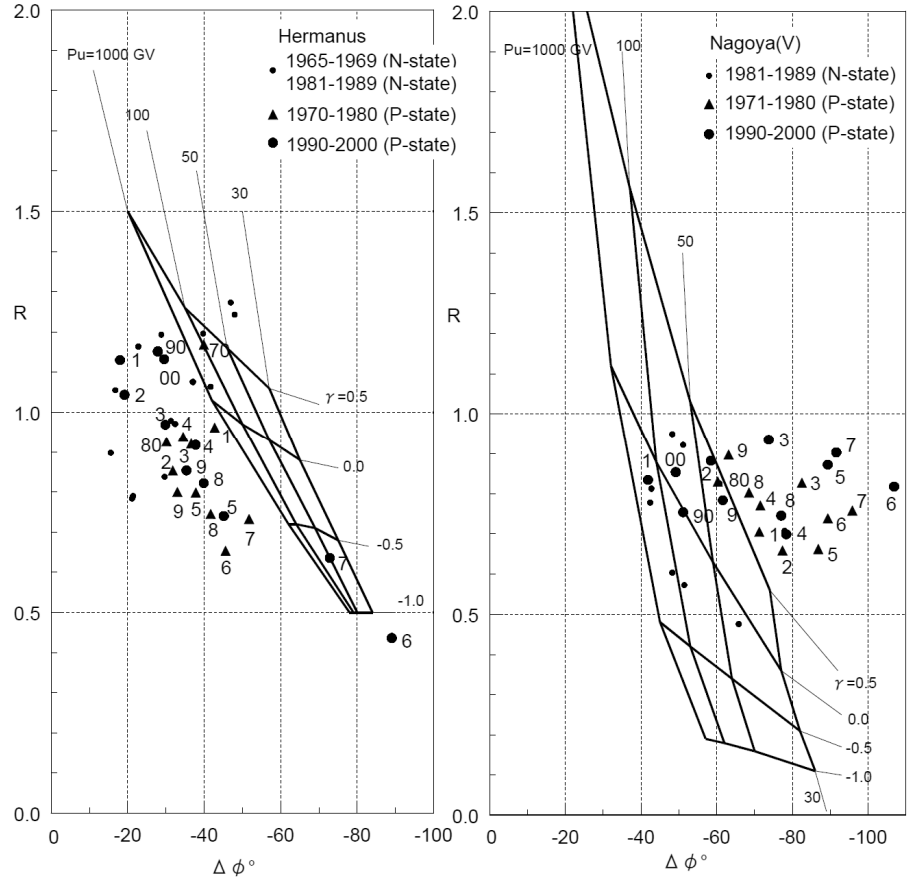

Fig. 30. R-$\Delta\phi$ diagram at Hermanus (34°S, 19°E; 4.9 GV) during 1965–2000 on the left and at Nagoya (35°N, 137°E; 11.5 GV) during 1971–2000 on the right (Nagashima *et al.*, 2010). Any point in the net area can be explained by the solar anisotropy $\mathbf{S_oD_1}$ with parameters γ and p_u at the point. The number attached to each point expresses the observation year in the '70s and '90s in the P-state.

the N-state is retarded toward ∼12 hours from the middle of the 3rd quadrant by the softening of $f(p)dp$ with a decrease of the solar activity and, as a result, $\mathbf{S_oD_1}(j)$ of the X-type changed to the Y-type and reduced only its magnitude without changing its phase (cf. Figs. 29 and 30). Similar phenomena to those at Nagoya were observed also at Huancayo ($\lambda = 12.0°$S, $p_c = 13.0$ GV), Tokyo (35.8°N, 11.5 GV) and Beijing (40.1°N, 8.9 GV).

On the contrary, $\mathbf{S_oD_1}$(Hermanus) belongs to the X-type and almost all the characteristic points on the R-$\Delta\phi$ diagram are in the left-outside region of the net area. Such a deviation from the net area is not attributable to statistical errors, as almost all the deviations are distributed in the left-side area with respect to the iso-p_u line of 10^3 GV. It is also noted that this area is forbidden, not only for the points derived from S_oA with the present spectrum form but also for those with any reasonable spectra as far as S_oA is an unidirectional form. Therefore, the distribution of the points is of the X-type and clearly indicates the existence of $\mathbf{S_oD_1^T}$. However, there are two exceptional points similar to the 3 exceptional cases at Nagoya, which show very small R's in the solar activity minimum periods (1996, '97) as $\mathbf{S_oD_1}$(Hermanus) of the X-type changed to the Y-type due to a phase shift toward ∼12 hours for a decrease of solar activity. It is emphasized that the appearance of these Y-type $\mathbf{S_oD_1^r}$s at the two stations were in the same Q-period but occurred in different polarity states. Hermanus observed them in the N-state, while Nagoya observed them in the P-state. This is due to the phase shift with decrease of solar activity from ∼18 hr to ∼12 hr at Hermanus in the P-state and from ∼15 hr to ∼12 hr at Nagoya in the N-state, showing a good agreement with the solar modulation of the phase of $\mathbf{S_oD_1}$ mentioned earlier (Munakata and Nagashima, 1986).

Such an influence of $\mathbf{S_oD^T}$ on the $\mathbf{S_oD_1}$ can be produced also by the seasonal variation $\mathbf{S_oD^H}$ with the phase ϕ_H of 0 hr local solar time caused by the seasonal variation of $\mathbf{HD_1}$ (cf. Nagashima *et al.*, 2010). Therefore, the resultant variation $\mathbf{S_oD_1^r}$ is expressed by

$$\mathbf{S_oD_1^r} = \mathbf{S_oD_1} + \mathbf{S_oD_1^T} + \mathbf{S_oD_1^H}. \tag{11}$$

It is emphasized that the influence of the sidereal anisotropies on the solar diurnal variation is not negligibly small.

7. Conclusion

The existence of CR sidereal anisotropies GA and TA was discovered in 1995 by the analysis of the observation of sidereal diurnal variations at the underground stations Hobart and Sakashita, and the ground station Nagoya, being incited by the casual finding of the seasonal variation of the sidereal diurnal variation at Hobart and also assisted by the acknowledged elimination method for the spurious sidereal variation produced by the CR solar anisotropy (cf.

Table 1). The discovery enabled a unified explanation to be offered at least qualitatively for those conflicting observed phenomena of the sidereal variations in the past.

The sidereal diurnal variations $G(t_{S_i})$ and $T(t_{S_i})$ produced by GA and TA and another one $H(t_{S_i})$ by HA (cf. Table 1) are subject, respectively, to the three kinds of HMS modulation characterized by the polarity reversal of the solar polar magnetic field with 22-years periodicity and the solar activity dependence with 11-years periodicity (cf. Table 1). These modulation patterns together with the theoretical modulation model of CRs in the spherical HMS can determine their origins; one (GA) is of galactic origin from $\alpha = 0$ hr and others (TA and HA) are, respectively, the sharply-concentrated CR fluxes along the neutral sheet of the HMS from $\alpha = 6$ hr and 18 hr. The sharp concentration of the anisotropies can be produced by applying the CR-Lens-Effect of the HMS to the accelerated CRs on the boundary of the HMS with the short nose and the long tail together with the wavy neutral sheet.

The duality of the motion of the HMS observed, respectively, by the CRs and the neutral particles suggests the existence of the proper motion $\mathbf{V_{IGM}}$ of the interstellar gaseous matter (IGM) including the magnetic field. $\mathbf{V^{CS}_{HMS}}$ produces the electromagnetic interaction between the HMS and IGM and forms the disturbed region surrounding the HMS, called the Subordinate HMS (S_uHMS), which prevents the C-G effect expected to be caused by the relative motion between the HMS and the low energy CRs in IGM. In the high-energy region, however, as CRs can freely pass through the IGM and the S_uHMS, the C-G effect can be observed in the direction of $\mathbf{V^{CS}_{HMS}}$ (not $\mathbf{V_{np}}$). On the other hand, as the neutral particles cannot recognize the existence of the S_uHMS owing to their long scattering mean free path compared with the scales of the S_uHMS, the particles can pass through the S_uHMS with the velocity $\mathbf{V_{IGM}}$ and produce the motion of $\mathbf{V_{np}}$ observed on the HMS. As above, the solar modulation of CR sidereal anisotropies are intimately correlated with the behavior pattern of the heliomagnetosphere (HMS) and also with the CR solar diurnal variation produced by the diffusion-convection process inside the HMS. One of the most remarkable results of the present analysis is that the motion ($\mathbf{V^{S}_{IGM}}$) of the interstellar gaseous matter (IGM) relative to the neighboring stars could be estimated for the first time by using the duality of the velocities $\mathbf{V^{CS}_{HMS}}$ and $\mathbf{V^{HMS}_{np}}$.

However, the sidereal anisotropies of CRs and their related phenomena are not completely solved yet, as they are based on basic assumptions such as the acceleration of CRs on the boundary of the HMS, the motion of IGM in space, the formation of the S_uHMS surrounding the HMS and so on. It is necessary to confirm these assumptions theoretically and experimentally not only for the sidereal anisotropies of CRs but also for the further development of the interaction between the HMS and the interstellar medium.

Acknowledgments. The authors express their sincere appreciation for the long-term continuous observations of cosmic ray diurnal variations performed with the neutron monitor network in the world by many researchers, with the ion chambers at Godhaven, Cheltenham, Huancayo and Christchurch by the Late Dr. S. E. Forbush and his colleagues, and at Yakutsk by the Late Professor Emeritus Yu. G. Shafer, Dr. G. B. Shafer and their colleagues, with the underground muon telescope at Cambridge, Hobart by the Late Drs. A. G. and K. B. Fenton, Dr. J. E. Humble and their colleagues, with the muon telescopes at Mawson, Antarctica by one of the authors (R. M. J.), Drs. J. E. Humble, M. L. Duldig and their colleagues and expeditionists, with the underground muon telescopes at Misato and Matsushiro by one of the authors (S. M.) and his colleagues, with the muon telescopes on the ground at Nagoya and the underground station at Sakashita by the Late Professors Emeritus Y. Sekido, K. Murakami and H. Ueno, the Late Dr. K. Fujimoto and their colleagues, with the air shower observation at Mt. Norikura (the University of Tokyo) by the Late Professor H. Ueno and his colleagues at Nagoya University and, finally, for the positive support for the data analysis of the World Data Center C2 for Cosmic Rays by the Late Dr. Y. Miyazaki, Dr. M. Wada, one of the authors (I. K.) and their colleagues. Without these observations and the analysis, the present result could not be obtained.

References

Abbasi, R. *et al.* (ICECUBE collaboration), Measurement of the anisotropy of cosmic ray arrival directions with IceCube, *Astrophys. J.*, **718**, L194–L198, 2010.

Abdo, A. A. *et al.*, Discovery of localized region of excess 10-TeV cosmic rays, *Phys. Rev. Lett.*, **101**, 221101–221105, 2008.

Ajello, J. M., An interpretation of Mariner 10 helium (584Å) and hydrogen (1216Å) interplanetary emission observations, *Astrophys. J.*, **222**, 1068–1079, 1978.

Alexeenko, V. V., A. E. Chudakov, E. N. Gulieva, and V. G. Sborshikov, Anisotropy of small E. A. S. ($\sim 10^{13}$ eV), *Proc. 17th Int. Cosmic Ray Conf.*, Paris, **2**, 146–149, 1981.

Alexeenko, V. V. and G. Navarra, Possible contribution of primary gamma-rays to the observed cosmic-ray anisotropy, *Lett. Nuovo Cimento*, **42**(7), 321–324, 1985.

Amenomori *et al.*, Observation of the multi-Tev cosmic-ray anisotropy due to the terrestrial orbital motion around the Sun in Tibet, *Phys. Rev. Lett.*, **93**(6), 61101–61104, 2004.

Amenomori *et al.*, Large-scale sidereal anisotropy of galactic cosmic-ray intensity observed by the Tibet air shower array, *Astrophys. J.*, **626**, L29–L32, 2005.

Andreyev, V. M., A. E. Chudakov, V. A. Kozyarivsky, A. M. Sidorenko, T. I. Tulupova, and A. V. Voevodsky, Cosmic ray sidereal anisotropy observed by Baksan underground scintillation telescope, *Proc. 20th Int. Cosmic Ray Conf.*, Moscow, **2**, 22–25, 1987.

Babcock, H. D., The Sun's polar magnetic field, *Astrophys. J.*, **130**, 364–365, 1959.

Beach, L. and S. E. Forbush, Cosmic-ray results, *C. I. W. Publ. 175*, Vol. XXI, Carnegie Inst. of Washington, Washington D.C., 1961.

Belov, A., Large scale modulation: View from the Earth, *Space Sci. Rev.*, **93**, 79–105, 2000.

Benko, G., K. Kecskemety, J. Kota, A. J. Somogyi, and A. Varga, Sidereal anisotropy of $\sim 10^{11}$ eV cosmic rays and interplanetary magnetic field directions, *Proc. of 16th Int. Cosmic Ray Conf.*, Kyoto, **4**, 205–209, 1979.

Bercovitch, M., The response of the cosmic ray sidereal diurnal variation to reversal of the solar magnetic field, *Proc. of International Symposium on Cosmic Ray Modulation in the Heliosphere*, Iwate Univ., Morioka, Japan, 329–336, 1984.

Bercovitch, M. and S. Agrawal, Cosmic ray anisotropies at median primary rigidities between 100 and 1000 GV, *Proc. 17th Int. Cosmic Ray Conf.*, Paris, **10**, 246–249, 1981.

Bieber, J. W. and M. A. Pomerantz, A unified theory of cosmic ray diurnal variation, *Geophys. Res. Lett.*, **10**, 920–923, 1983.

Campbell, W. W. and J. H. Moore, Review of publications (Stellar Radial Velocities. Publications of the Lick Observatory, Vol. XVI), *J. R. Astron. Soc. Can.*, **22**, 148–151, 1928.

Cini-Castagnoli, G., D. Marocchi, H. Elliot, R. G. Marsden, and T. Thambyahpillai, Change in the phase of the apparent sidereal variation, *Proc. 14th Int. Cosmic Ray Conf.*, Munich, **4**, 1453–1457, 1975.

Compton, A. H. and I. A. Getting, An apparent effect of galactic rotation on the intensity of cosmic rays, *Phys. Rev.*, **47**, 817–821, 1935.

Conforto, A. M. and J. A. Simpson, The 24 hour intensity variations of the primary cosmic rays, *Il Nuovo Cimento*, **6**, 1052–1063, 1957.

Cutler, D. J. and D. E. Groom, Mayflower mine 1500 GV detector; cosmic ray anisotropy and search for Cygnus X-3, *Astrophys. J.*, **376**, 322–334,

1991.
Davies, S. T., H. Elliot, and T. Thambyahpillai, Sidereal anisotropy and Sun's magnetic field, *Proc. 15th Int. Cosmic Ray Conf.*, Plovdiv, **4**, 105–110, 1977.
Davies, S. T., H. Elliot, R. G. Marsden, T. Thambyahpillai, and J. C. Dutt, The angular distribution of cosmic rays at the boundary of the heliosphere, *Planet. Space Sci.*, **27**, 733–738, 1979.
Davis, L., Jr., Anisotropy of high-energy cosmic rays, *Phys. Rev.*, **96**, 743–751, 1954.
Davis, L., Jr., Interplanetary magnetic fields and cosmic rays, *Phys. Rev.*, **100**, 1440–1444, 1955.
Dorman, L. I., Cosmic ray variations, *State Publishing House for Technical and Theoretical Literature*, Moscow, 1957.
Duldig, M. L., Heliospheric modulation: Theory and underground observations, *ANARE RESEARCH NOTES*, Department of the Environment and Heritage, Channel Highway, Kingston, Tasmania 7050, Australia, 145, 2000.
Duperier, A., A new cosmic-ray recorder and the air-absorption and decay of particles, *Terr. Mag. Atmos. Elect.*, **49**, 1–7, 1944.
Duperier, A., Solar and sidereal diurnal variations of cosmic rays, *Nature*, **158**, 196–196, 1946.
Duperier, A., Latitude effect and pressure-level of meson formation, *Nature*, **163**, 369–370, 1949.
Elliot, H., Time variations of cosmic ray intensity, *Prog. in Cosmic Ray Phys.*, North-Holland Publ. Co., Amsterdam, **1**, 453–514, 1952.
Farley, F. J. M. and J. R. Storey, The sidereal correlation of extensive air showers, *Proc. Phys. Soc. A*, **67**, 996–1004, 1954.
Fenton, A. G. and K. B. Fenton, Sidereal cosmic ray variations at ∼365 m.w.e. underground, *Proc. 14th Int. Cosmic Ray Conf.*, Munich, **4**, 1482–1485, 1975.
Fenton, A. G. and K. B. Fenton, Sidereal cosmic ray variations at 365 M.W.E. underground, *Proc. Int. Cosmic Ray Sympo. High Energy Cosmic Ray Modulation*, 313–315, 1976.
Fenton, A. G., K. B. Fenton, J. E. Humble, K. Bolton, R. M. Jacklyn, M. L. Duldig, K. Murakami, Z. Fujii, T. Yamada, S. Sakakibara, K. Fujimoto, H. Ueno, and K. Nagashima, Sidereal anisotropy of cosmic rays with median energy 70 TeV observed at Liawenee, Tasmania, *Proc. 21st Int. Cosmic Ray Conf.*, Adelaide, **3**, 177–179, 1990.
Fenton, K. B., A. G. Fenton, and J. E. Humble, Sidereal variations at high energies—observations at Poatina, *Proc. 24th Int. Cosmic Ray Conf.*, Rome, **4**, 635–638, 1995.
Forbush, S. E., On diurnal variation in cosmic-ray intensity, *Terr. Magn. Atmos. Electr.*, **42**, 1–16, 1937a.
Forbush, S. E., On sidereal diurnal variation in cosmic-ray intensity, *Phys. Rev.*, **52**, 1254–1256, 1937b.
Forbush, S. E., World-wide changes in cosmic-ray intensity, *Rev. Mod. Phys.*, **11**, 168–172, 1939.
Fujii, Z., H. Ueno, S. Mori, and K. Nagashima, Sidereal semi-diurnal variations observed at Nagoya, Misato and Sakashita stations, *Proc. of International Symposium on Cosmic Ray Modulation in the Heliosphere*, Iwate Univ., Morioka, Japan, 364–371, 1984.
Fujimoto, K., A. Inoue, K. Murakami, and K. Nagashima, Coupling coefficients of cosmic ray daily variations for meson telescopes, *Report of Cosmic-Ray Research Laboratory*, No. 9, Cosmic-Ray Research Laboratory, Nagoya Univ., Nagoya, Japan, 1984.
Gavril'yev, A. I., P. A. Krivoshapkin, A. I. Kuzmin, G. V. Skripin, and V. A. Filippov, Stellar-daily cosmic-ray variation, *Geomagn. Aeron.*, **17**, 257–259, 1977.
Gleeson, L. J. and W. I. Axford, Cosmic rays in the interplanetary medium, *Astrophys. J.*, **149**, L115–L118, 1967.
Gombosi, T., J. Kota, A. J. Somogyi, A. Varge, B. Betev, L. Katsarski, S. Kavlalov, and I. Khirov, Galactic cosmic ray anisotropy at $\approx 6 \cdot 10^{13}$ eV, *Proc. 14th Int. Cosmic Ray Conf.*, Munich, **2**, 586–591, 1975.
Guillian, G. *et al.* (The Super-Kamiokande Collaboration), Observation of the anisotropy of 10 TeV primary cosmic ray nuclie flux with the Super-Kamiokande-I detector, *Phys. Rev.*, **D75**, 062003–062019, 2007.
Hall, D. L., K. Munakata, S. Yasue, S. Mori, C. Kato, M. Koyama, S. Akahane, Z. Fujii, K. Fujimoto, J. E. Humble, A. G. Fenton, K. B. Fenton, and M. L. Duldig, Preliminary analysis of two hemisphere observations of sidereal anisotropies of galactic cosmic rays, *J. Geophys. Res.*, **103**(A1), 367–372, 1998.
Hall, D. L., K. Munakata, S. Yasue, S. Mori, C. Kato, M. Koyama, S. Akahane, Z. Fujii, K. Fujimoto, J. E. Humble, A. G. Fenton, K. B. Fenton, and M. L. Duldig, Gaussian analysis of two hemisphere observations of galactic cosmic ray sidereal anisotropies, *J. Geophys. Res.*, **104**(A4), 6737–6749, 1999.
Howard, R., Studies of solar magnetic fields I. The average field strengths, *Sol. Phys.*, **38**, 283–299, 1974a.
Howard, R., Studies of solar magnetic fields II. The magnetic fluxes, *Sol. Phys.*, **38**, 59–67, 1974b.
Humble, J. E. and A. G. Fenton, Sidereal variations observed underground in Tasmania, *Proc. 14th Int. Cosmic Ray Conf.*, Munich, **12**, 4226–4228, 1975.
Humble, J. E., A. G. Fenton, and K. B. Fenton, Sidereal variations deep underground in Tasmania, *Proc. 19th Int. Cosmic Ray Conf.*, La Jolla, **5**, 39–41, 1985.
Ichinose, M. and K. Murakami, Sidereal time variation of cosmic rays, *Proc. of International Cosmic Ray Symposium on High Energy Cosmic Ray Modulation*, 291–296, Tokyo Univ., Japan, 1976.
Inoue, A., M. Wada, and I. Kondo, Cosmic ray tables No. 1 Asymptotic directions in 1975, *World Data Center C2 for Cosmic Rays*, Institute of Physical and Chemical Research, Itabashi, Tokyo, March, 1983.
Jacklyn, R. M., The barometer coefficient and air mass effects on cosmic rays at Macquarie Island, *Aust. J. Phys.*, **7**, 315–321, 1954.
Jacklyn, R. M., The apparent sidereal and anti-sidereal daily variations of cosmic ray intensity, *Il Nuovo Cimento*, **24**, 1034–1065, 1962.
Jacklyn, R. M., Evidence for a two-way sidereal anisotropy in the charged primary cosmic radiation, *Nature*, **211**, 690–693, 1966.
Jacklyn, R. M., Underground studies in Tasmania and at Mawson, *ANARE RESEARCH NOTES*, Department of the Environment and Heritage, Channel Highway, Kingston, Tasmania 7050, Australia, **102**, 91–101, 2000.
Jokipii, J. R. and D. A. Kopriva, Effects of particle drift on the transport of cosmic rays, III Numerical models of galactic cosmic-ray modulation, *Astrophys. J.*, **234**, 384–392, 1979.
Kota, J., On the second spherical harmonics of the cosmic ray angular distribution, *J. Phys.*, **A8**, 1349–1360, 1975.
Kota, J. and J. R. Jokipii, Effects of drift on the transport of cosmic rays, A three-dimensional model including diffusion, *Astrophys. J.*, **265**, 573–581, 1983.
Krainev, M. B., The electromagnetic field in and outside the solar wind cavity and the galactic cosmic rays, *Proc. 17th Int. Cosmic Ray Conf.*, Paris, **3**, 357–360, 1981.
Kuzmin, A. I., P. A. Krivoshapkin, A. I. Gavrilyev, G. V. Skripin, V. A. Filippov, and A. N. Prikhodko, Change of cosmic ray anisotropy with solar activity cycle (abstract), *Proc. 15th Int. Cosmic Ray Conf.*, Plovdiv, **3**, 156–156, 1977.
Lange, I. and S. E. Forbush, Cosmic ray results from Huancaya observatory, Peru, June 1936-December 1946, *Researches of the Dept. Terrestrial Magnetism, C. I. W. Publ. 175*, Vol. XIV, Carnegie Inst. of Washington, Washington D.C., 1948.
Lange, I. and S. E. Forbush, Cosmic ray results, *Researches of the Dept. Terrestrial Magnetism, C. I. W. Publ. 175*, Vol. XX, Carnegie Inst. of Washington, Washington D.C., 1957.
Lee, T. W. and L. K. Ng, Observation of cosmic-ray intensity variation using an underground telescope, *Proc. 20th Int. Cosmic Ray Conf.*, Moscow, **2**, 18–21, 1987.
Marsden, R. G., H. Elliot, R. J. Hynds, and T. Thambyahpillai, The directional dependence of the primary cosmic rays of energies 10^{11}–10^{12} eV, *Nature*, **260**, 491–495, 1976.
McClintock, W., R. C. Henry, J. L. Linsky, and H. W. Moos, Ultraviolet observations of cool stars. VII. Local interstellar hydrogen and deuterium lyman-alpha, *Astrophys. J.*, **225**, 465–481, 1978.
Moraal, H., Observations of the eleven-year cosmic ray modulation cycle, *Space Sci. Rev.*, **19**, 845–920, 1976.
Mori, S., D. B. Swinson, K. Fujimoto, and K. Nagashima, 22-year variation in the solar diurnal anisotropy of cosmic rays, *Proc. 17th Int. Cosmic Ray Conf.*, Paris, **10**, 218–221, 1981.
Mori, S., S. Yasue, S. Sagisaka, M. Ichinose, K. Chino, S. Akahane, and T. Higuchi, Matsushiro underground cosmic-ray observatory (220 m.w.e. depth) and the observation of high energy ($<10^{12}$ eV) cosmic ray intensity variation, *J. Fac. Sci. Shinshu Univ.*, Matsumoto, Japan, **24**(1), 1–54, 1989.
Mori, S., S. Yasue, K. Munakata, M. Koyama, Y. Shiozaki, Y. Yokota, S. Akasofu, Z. Fujii, I. Morishita, J. E. Humble, A. G. Fenton, K. B. Fenton, and M. L. Duldig, Two hemisphere observations of the north-south sidereal asymmetry at ∼1 TeV, *Proc. 23rd Int. Cosmic Ray Conf.*, Calgary, **3**, 656–659, 1993.
Munakata, K. and K. Nagashima, A theory of cosmic ray anisotropies of solar origin, *Planet. Space Sci.*, **34**, 99–116, 1986.
Myssowsky, L. and L. Tuwim, Absorption in Blei, sekundäre Strahlen und Wellenlänge der Höhenstrahlung, *Zeit. Phys.*, **50**, 273–292, 1928.

Nagashima, K., Long term modulation of cosmic rays in heliomagnetosphere, *Proc. 15th Int. Cosmic Ray Conf.*, Plovdiv, **10**, 380–396, 1977.

Nagashima, K., Long term modulation of galactic cosmic rays, *Proc. 21st Int. Cosmic Ray Conf.*, Adelaide, **11**, 207–226, 1990.

Nagashima, K. and Z. Fujii, Coexistence of cosmic-ray sidereal anisotropies originating in galactic space and at the heliomagnetospheric nose and tail boundaries, observed with muon detectors in the energy region of 60∼100 GeV, *Earth Planets Space*, **58**, 1487–1498, 2006.

Nagashima, K. and S. Mori, Summary of general discussion on sidereal daily variation of high energy cosmic rays, *Proc. of International Cosmic Ray Symposium on High Energy Cosmic Ray Modulation*, Tokyo Univ., Japan, 326–360, 1976.

Nagashima, K. and I. Morishita, Long term modulation of cosmic rays and inferable electromagnetic state in solar modulation region, *Planet. Space Sci.*, **28**, 177–194, 1980a.

Nagashima, K. and I. Morishita, Twenty-two year modulation of cosmic rays associated with polarity reversal of polar magnetic field of the Sun, *Planet. Space Sci.*, **28**, 195–205, 1980b.

Nagashima, K. and I. Morishita, Cosmic ray sidereal variation of galactic origin observable in the heliomagnetosphere, *Report of Cosmic-Ray Research Lab.*, No. 8, Cosmic-Ray Research Laboratory, Nagoya Univ., Nagoya, Japan, 1983 (Ref. 2).

Nagashima, K. and H. Ueno, Three-dimensional cosmic ray anisotropy in interplanetary space, 2, General expression of annual modulation of daily variation by frequency modulation method and its application to the modulation due to Earth's revolution around Sun, *Rep. Ionos. Space Res. Jpn.*, **25**, 212–241, 1971.

Nagashima, K., H. Ueno, S. Mori, and S. Sagisaka, A two-way sidereal anisotropy, *Can. J. Phys.*, **46**, S611–S613, 1968.

Nagashima, K., I. Morishita, and S. Yasue, Modulation of galactic cosmic ray anisotropy in heliomagnetosphere: Average sidereal daily variation, *Planet. Space Sci.*, **30**, 879–896, 1982 (Ref. 1).

Nagashima, K., Y. Ishida, S. Mori, and I. Morishita, Cosmic ray sidereal diurnal variation of galactic origin observed by neutron monitors, *Planet. Space Sci.*, **31**, 1269–1278, 1983a.

Nagashima, K., R. Tatsuoka, and S. Matsuzaki, Spurious sidereal daily variation of cosmic rays produced from stationary anisotropy of solar origin, *Il Nuovo Cimento*, **C6**, 550–565, 1983b.

Nagashima, K., Y. Ishida, S. Mori, and I. Morishita, Cosmic ray sidereal diurnal variation of galactic origin observed by neutron monitors, *Proc. of International Symposium on Cosmic Ray Modulation in the Heliosphere*, Iwate Univ., Morioka, Japan, 343–348, 1984.

Nagashima, K., S. Sakakibara, A. G. Fenton, and J. E. Humble, The insensitivity of the cosmic ray galactic anisotropy to heliomagnetic polarity reversal, *Planet. Space Sci.*, **33**, 395–405, 1985.

Nagashima, K., R. Tatsuoka, and K. Munakata, Dependence of cosmic ray solar daily variation (1st, 2nd, and 3rd) on the heliomagnetic polarity reversals, *Planet. Space Sci.*, **34**, 469–482, 1986.

Nagashima, K., K. Fujimoto, S. Sakakibara, Z. Fujii, H. Ueno, I. Morishita, and K. Murakami, Galactic cosmic-ray anisotropy and its modulation in the heliomagnetosphere, inferred from air shower observation at Mt. Norikura, *Il Nuovo Cimento*, **12C**(6), 695–749, 1989.

Nagashima, K., K. Fujimoto, and R. Tatsuoka, Nature of solar-cycle and heliomagnetic polarity dependence of cosmic rays, Inferred from their correlation with the heliomagnetic spherical harmonics in the period 1976-1985, *Planet. Space Sci.*, **39**, 1617–1635, 1991.

Nagashima, K., K. Fujimoto, and R. M. Jacklyn, The excess influx of galactic cosmic rays from the tailend side of the heliomagnetosphere, inferred from their sidereal daily variation, *Proc. Mini Int. Conf. Solar Particle Physics and Cosmic Ray Modulation*, 93–98, STE Lab. Nagoya Univ., Nagoya, Japan, 1995a.

Nagashima, K., K. Fujimoto, and R. M. Jacklyn, Cosmic ray sidereal variation of the coexistence of the galactic and heliomagneto tail-in anisotropies, *Proc. 24th Int. Cosmic Ray Conf.*, Rome, **4**, 652–655, 1995b.

Nagashima, K., K. Fujimoto, and R. M. Jacklyn, Cosmic-ray excess flux from heliomagneto tail, *Proc. of 24th Int. Cosmic Ray Conf.*, Rome, **4**, 656–659, 1995c.

Nagashima, K., K. Fujimoto, and R. M. Jacklyn, Galactic and heliotail-in anisotropies of cosmic rays as the origin of sidereal daily variation in the energy region $<10^4$ GeV, *J. Geophys. Res.*, **103**, 17429–17440, 1998 (Ref. 3).

Nagashima, K., Z. Fujii, and K. Munakata, Solar modulation of galactic and heliotail-in anisotropies of cosmic rays at Sakashita underground station (320∼650 GeV), *Earth Planets Space*, **56**, 479–483, 2004.

Nagashima, K., I. Kondo, and Z. Fujii, Sharply concentrated cosmic-ray excess fluxes from heliomagnetospheric nose and tail boundaries observed with neutron monitors on the ground, *Earth Planets Space*, **57**, 1083–1091, 2005.

Nagashima, K., I. Kondo, I. Morihsita, and R. M. Jacklyn, The influence of the sidereal cosmic-ray anisotropies originated on the tail- and nose-boundaries of the heliomagnetosphere (HMS) upon the solar cosmic-ray anisotropy produced inside the HMS, *Earth Planets Space*, **62**, 525–544, 2010.

Olbert, S., Atmospheric effects on cosmic-ray intensity near sea level, *Phys. Rev.*, **92**, 454–461, 1953.

Sarabhai, V. and G. Subramanian, Galactic cosmic rays in the solar system, *Astrophys. J.*, **145**, 206–214, 1966.

Schatten, K. H. and J. M. Wilcox, Direction of Nearby galactic magnetic field inferred from a cosmic-ray diurnal anisotropy, *J. Geophys. Res.*, **74**, 5157–4161, 1969.

Sekido, Y., Cosmic rays on the Pacific Ocean. Part II. On the barometer effect of cosmic rays, *Sci. Pap. Inst. Phys. Chem. Res.*, **40**, 456–466, 1943.

Sekido, Y., K. Nagashima, I. Kondo, T. Murayama, H. Ueno, S. Sakakibara, and K. Fujimoto, Sidereal time variation of high-energy cosmic rays observed by an air Cerenkov telescope, *Can. J. Phys.*, **46**, S607–610, 1968.

Sekido, Y., K. Nagashima, I. Kondo, and S. Sakakibara, Sidereal and solar anisotropy of high-energy cosmic rays observed by an air Cerenkov telescope, *Proc. 12th Int. Cosmic Ray Conf.*, Hobart, **1**, 302–307, 1971.

Shafer, G. B. and Yu. G. Shafer, Precise observation of cosmic rays at Yakutsk, *Inst. Cosmophys. Res. Aeron.*, Yakutsk, Science Academy of USSR, 1984.

Speller, R., T. Thambyahpillai, and H. Elliot, Cosmic ray isotropy and the origin problem, *Nature*, **235**, 25–29, 1972.

Swinson, D. B., Field dependent cosmic ray streaming at high rigidities, *J. Geophys. Res.*, **81**, 2075–2081, 1976.

Swinson, D. B. and K. Nagashima, Corrected sidereal anisotropy for underground muons, *Planet. Space Sci.*, **33**, 1069–1072, 1985.

Tatsuoka, R. and K. Nagashima, Formulation of cosmic-ray solar daily variation and its seasonal variation, produced from generalized stationary anisotropy of solar origin, *Il Nouvo Cimento*, **C8**, 320–328, 1985.

Thambyahpillai, T., The sidereal diurnal variations measured underground station in London, *Proc. 18th Int. Cosmic Ray Conf.*, Bangalore, **3**, 383–386, 1983.

Thambyahpillai, T. and H. Elliot, World-Wide Changes in the phase of the cosmic-ray solar daily variation, *Nature*, **171**, 918–920, 1953.

Trefall, H., On the barometer effect on the hard component of the cosmic radiation, *Proc. Phys. Soc. Lond.*, **A68**, 953–961, 1955.

Ueno, H., Z. Fujii, S. Mori, S. Yasue, and K. Nagashima, Sidereal diurnal variations observed at Nagoya, Misato, and Sakashita stations (NAMS), *Proc. of International Symposium on Cosmic Ray Modulation in the Heliosphere*, Iwate Univ., Morioka, Japan, 349–354, 1984.

Ueno, H., Z. Fujii, and T. Yamada, 11 years variations of sidereal anisotropy observed at Sakashita underground station, *Proc. 21st Int. Cosmic Ray Conf.*, Adelaide, **6**, 361–364, 1990.

Venkatesan, D. and R. S. Badruddin, Cosmic-ray intensity variations in the 3-dimensional heliosphere, *Space Sci. Rev.*, **52**, 121–194, 1990.

Wada, M., Atmospheric effects on the intensity of cosmic-ray mesons, (1) The barometer effect, *Sci. Pap. Inst. Phys. Chem. Res.*, **54**(5), 335–352, 1960.

Yasue, S., S. Mori, S. Sakakibara, and K. Nagashima, Coupling coefficients of cosmic ray daily variations for neutron monitor stations, *Report of Cosmic-Ray Research Laboratory*, No. 7, Cosmic-Ray Research Laboratory, Nagoya Univ., Nagoya, Japan, 1982.

Yasue, S., I. Morishita, and K. Nagashima, Modulation of galactic cosmic-ray anisotropy in heliomagnetosphere: Influence of cosmic-ray scattering on sidereal daily variation, *Planet. Space Sci.*, **33**, 1057–1068, 1985.

K. Nagashima, I. Morishita (e-mail: isao@alice.asahi-u.ac.jp), Z. Fujii, S. Mori, I. Kondo, and R. M. Jacklyn